# 1 Inorganic Chemistry Basics

## 1.1 Introduction

No description of the metal-containing compounds that have found their way into medicine would be useful without first providing basic information on the bonding in metal complexes, their spectral and magnetic properties and, most importantly, the manner in which they react with water and biological targets in the cell. The approach taken in this chapter assumes background knowledge of general and organic chemistry with no previous exposure to inorganic chemistry, as would occur in a junior- or senior-level course at most universities. The concepts presented are for the most part intuitive, requiring basic knowledge of chemistry and physics, but sometimes more abstract issues like quantum mechanics – which explains the spectral properties of metal complexes – will also need to be covered. The overall goal of this chapter is to bring all readers to a common level, providing them with the 'core' of information needed to understand how and why, from the chemical perspective, metal complexes play important roles in medicine.

## 1.2 Crystal Field Theory

The bonding that exists in metal complexes, their spectral and magnetic properties and their chemical reactivity are not easily explained using a single theory. However, one approach that is often used in a basic presentation of bonding concepts in transition metal chemistry is crystal field theory (abbreviated CF theory), which because it is based on simple electrostatic arguments, is relatively easy to understand. In CF theory, the interactions between the metal ion (M) and the groups attached to it (called ligands and denoted by L) are considered to be electrostatic in nature, and the bonding in the compound is described as being salt-like in character. The metal ion, a *cation*, electrostatically interacts with a series of surrounding ligands, which are usually negatively charged or, if they are uncharged, have the negative end of a dipole directed toward the metal ion. Barring any serious steric interactions between the ligands, the arrangements about the metal ion generally have high-symmetry geometries. For example, a six-coordinate complex – that is, a compound with six ligands attached to the metal ion – has an octahedral arrangement of ligands, while five-coordinate complexes have square or trigonal bipyramidal arrangements, four-coordinate structures are tetrahedral and square planar, and so on. These geometries, along with compounds and intermediates commonly encountered in metal complexes used in medicine, are shown in Figure 1.1.

*Metals in Medicine*, Second Edition. James C. Dabrowiak.

Companion website: www.wiley.com/go/dabrowiak/metals2e

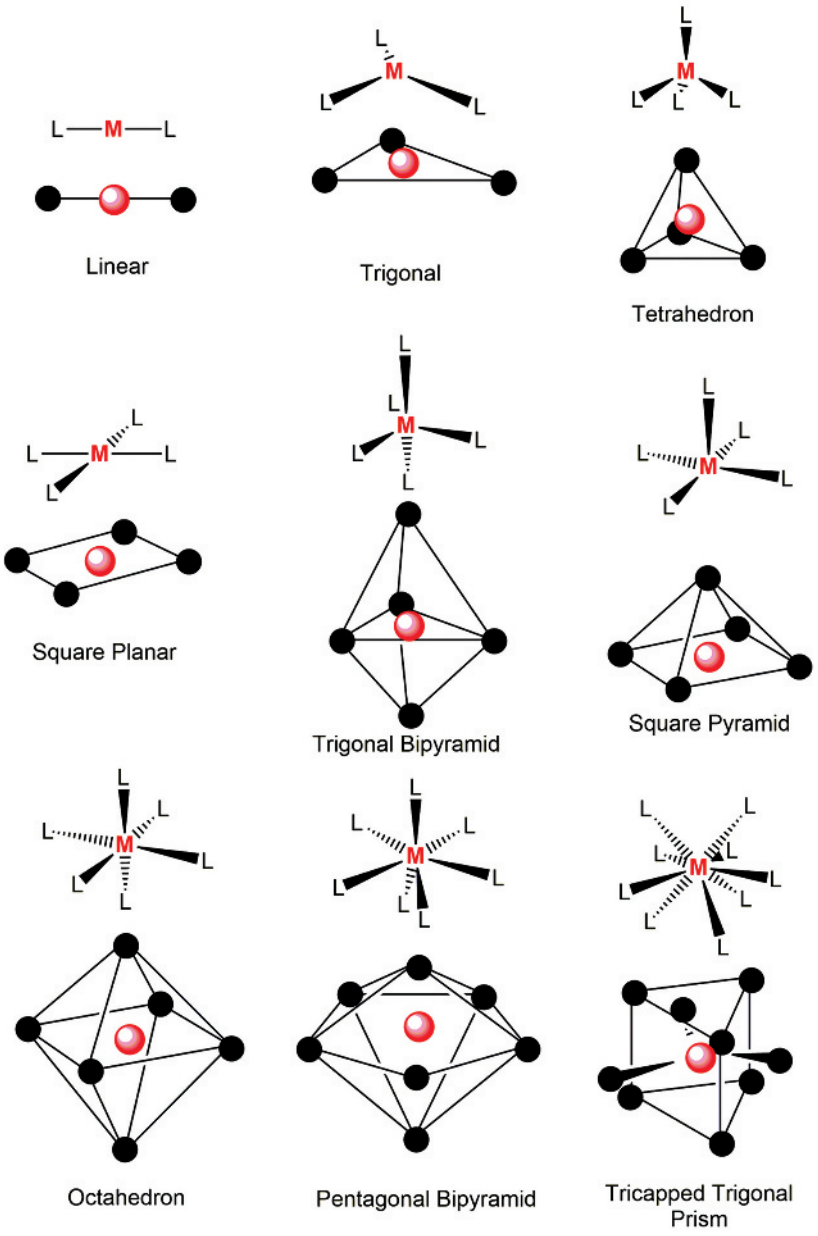


**Figure 1.1**
Common geometries of metal complexes and intermediates found in inorganic chemistry.

### 1.2.1 Octahedral Crystal Field

The first-row transition metal series, which begins with scandium, Sc, fills the 3*d* level of the atom, while the second- and third-row transition metal series, which begin with yttrium, Y, and lanthanum, La, respectively, fill the 4*d* (second row) and 5*d* (third row) orbitals of the atom. The transition metal ions and the electronic configurations of common oxidation

| | 3<br>3B | 4<br>3B | 5<br>5B | 6<br>6B | 7<br>7B | 8<br>8B | 9<br>8B | 10<br>8B | 11<br>1B | 12<br>2B |
|---|---|---|---|---|---|---|---|---|---|---|
| Ions | +2, $d^1$<br>+3, $d^0$ | +2, $d^2$<br>+3, $d^1$<br>+4, $d^0$ | +2, $d^3$<br>+3, $d^2$<br>+4, $d^1$<br>+5, $d^0$ | +2, $d^4$<br>+3, $d^3$<br>+4, $d^2$<br>+5, $d^1$<br>+6, $d^0$ | +1, $d^6$<br>+2, $d^5$<br>+3, $d^4$<br>+4, $d^3$<br>+5, $d^2$<br>+6, $d^1$<br>+7, $d^0$ | +2, $d^6$<br>+3, $d^5$<br>+4, $d^4$ | +2, $d^7$<br>+3, $d^6$<br>+4, $d^5$ | +2, $d^8$<br>+3, $d^7$<br>+4, $d^6$ | +1, $d^{10}$<br>+2, $d^9$<br>+3, $d^8$ | +2, $d^{10}$ |
| 1st Row $3d^n$ | $^{21}$Sc | $^{22}$Ti | $^{23}$V | $^{24}$Cr | $^{25}$Mn | $^{26}$Fe | $^{27}$Co | $^{28}$Ni | $^{29}$Cu | $^{30}$Zn |
| 2nd Row $4d^n$ | $^{39}$Y | $^{40}$Zr | $^{41}$Nb | $^{42}$Mo | $^{43}$Tc | $^{44}$Ru | $^{45}$Rh | $^{46}$Pd | $^{47}$Pd | $^{48}$Cd |
| 3rd Row $5d^n$ | $^{57}$La | $^{72}$Hf | $^{73}$Ta | $^{74}$W | $^{75}$Re | $^{76}$Os | $^{77}$Ir | $^{78}$Pt | $^{79}$Au | $^{80}$Hg |

**Figure 1.2**

Transition metal ions and their electronic configurations for various oxidation states.

states are shown in Figure 1.2. Since ions of these elements have electron occupancies in the *d* level, which is considered the 'valence' level of the ion, CF theory focuses on the change in energy of the *d-orbitals* when charges representing the ligands approach the metal ion and form salt-like bonds.

The spatial arrangements of the five *d*-orbitals on a Cartesian coordinate system are shown in Figure 1.3. The shapes shown represent the probability of finding an electron in a volume of space about the nucleus of the metal ion. If the metal ion has no bonded ligands – this is referred to as a *free* ion – the energies of all five *d*-orbitals will be the same and are said to be *five-fold degenerate* in energy. This situation is shown on the left side of Figure 1.4. Let's suppose that instead of existing as a free ion, the metal ion is part of a stable complex consisting of six negatively charged ligands bound to the metal ion in an octahedral array. The way that crystal field theory approaches this situation is to consider what happens to the five *d*-orbitals in the electrostatic field set that is up by the ligands. The first thing that the theory does is to consider a situation in which the total negative charge of the ligands is 'smeared' equally over the surface of a sphere with a radius equal to the metal–ligand bond distance and with the metal ion at its center. Since the *d*-orbitals have electrons in them and the surface of the sphere is negatively charged, the energies of the *d*-orbitals will be raised; that is, they will become less stable relative to the free ion, due to electrostatic repulsion between the d-electrons and the negatively charged surface of the sphere. Since the charge on the sphere has no 'directionality' – that is, the negative charges are equally distributed over the entire surface of the sphere – all five *d*-orbitals must experience the same electrostatic perturbation from the sphere and move as a group to a new energy, $E_o$ (see Figure 1.4). The next step is to redistribute the charge on the surface of the sphere and concentrate it at the six points where the axes penetrate the sphere. If the charge at each of

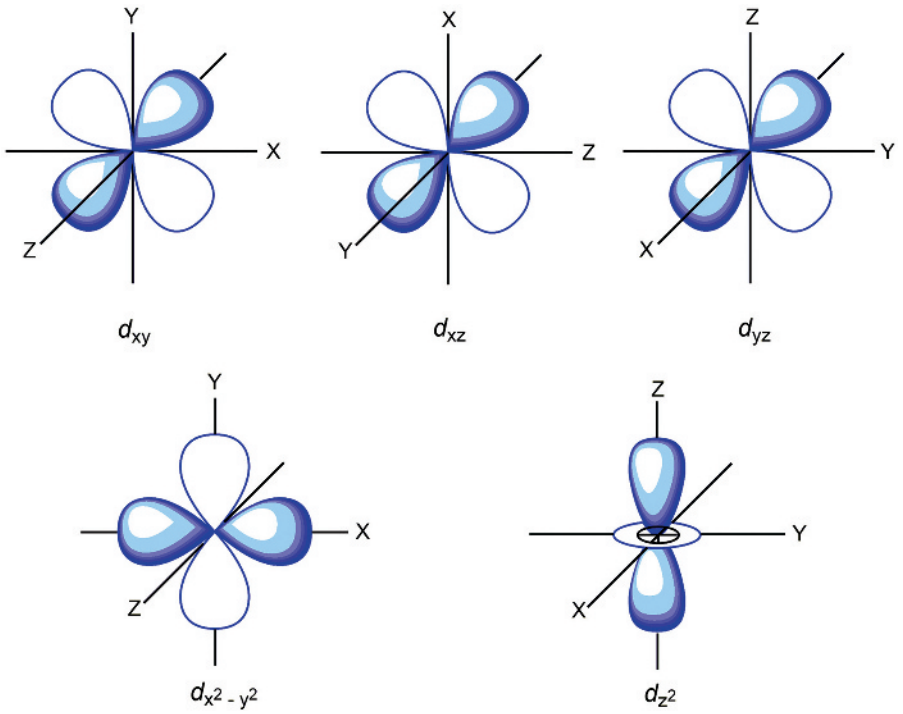


**Figure 1.3**
Boundary surfaces of the five *d*-orbitals.

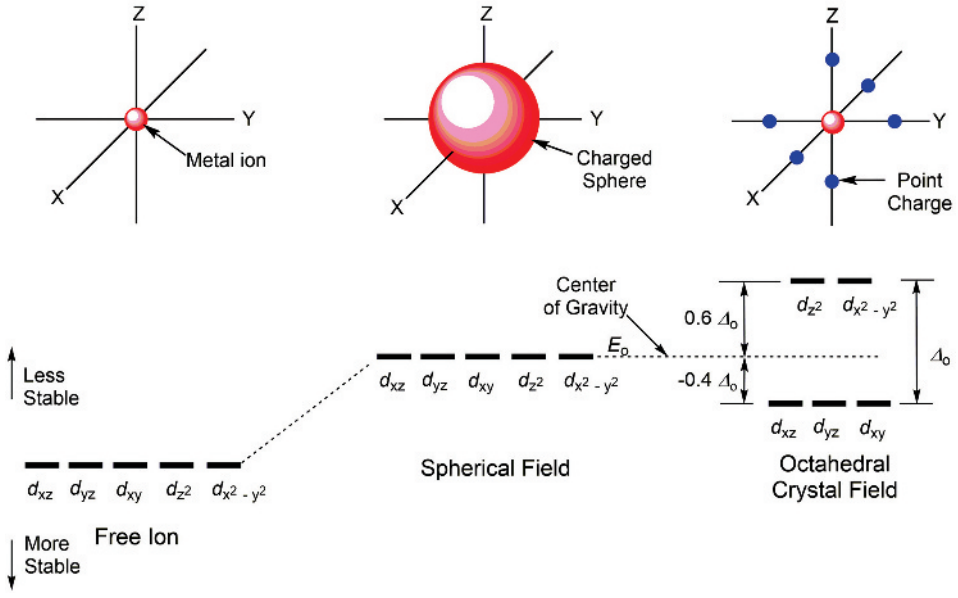


**Figure 1.4**
Generation of the octahedral crystal field from the free ion.

the six points is identical, this will produce a perfect octahedral crystal field about the central metal ion and simulate what the *d*-orbitals experience in an octahedral metal complex. It should be evident that since $d_{x^2-y^2}$ and $d_{z^2}$ are pointed directly at the charges (ligands), they must experience a different perturbation than the three orbitals, $d_{xz}$, $d_{yz}$, $d_{xy}$, that are directed between the charges. While it may not be obvious that both $d_{x^2-y^2}$ and $d_{z^2}$ should experience an identical perturbation from the octahedral field, quantum mechanics shows that $d_{z^2}$, which has a ring of electron density in the xy plane (Figure 1.3), is actually a composite of two orbitals that are identical to $d_{x^2-y^2}$, except that they lie in the yz and xz planes. Thus, since $d_{z^2}$ is a composite of two orbitals that look like $d_{x^2-y^2}$, it makes sense that the crystal field will affect $d_{z^2}$ and $d_{x^2-y^2}$ identically, as shown in Figure 1.4. It should also be evident that since these orbitals are pointed directly at the ligands, they feel the electrostatic repulsion directly, and thus their energies are *raised* relative to the energy of the spherical field, $E_o$. It is possible to show that if the total charge on the sphere is simply rearranged or 'localized' to certain positions on the sphere, the energy of the system cannot change; that is, $E_o$ for the sphere and the octahedral field must be the same. This is the *center of gravity* rule, which applies to electrostatic models of this type. The consequences of this is that if two orbitals, $d_{x^2-y^2}$ and $d_{z^2}$, are raised by a certain amount, the remaining three, $d_{xz}$, $d_{yz}$, $d_{xy}$, must be *lowered* by a certain amount. Inspection of the shapes and orientations of $d_{xz}$, $d_{yz}$, $d_{xy}$ shows that since these orbitals are directed 45° to the axes of the system, and each is related to the others by a simple rotation, all must experience exactly the same perturbation from the charges which are on the axes of the system. This set of orbitals, which are 'triply degenerate', is often referred to as the '$t_{2g}$' set due to its symmetry properties. In a similar fashion, the orbitals, $d_{x^2-y^2}$ and $d_{z^2}$ which are 'doubly degenerate' are referred to as the '$e_g$' set. The labels $t_{2g}$ and $e_g$ are products of the application of *group theory*, a mathematical tool for characterizing the symmetry properties of molecules.

Simple electrostatic arguments show that the spacing between the $t_{2g}$ and $e_g$ levels depends on the distance that the charge is from the origin of the system and the magnitude of the charge. If the distance is decreased, or if the magnitude of the negative charge is increased, the splitting between $t_{2g}$ and $e_g$ will increase. As we will see, metal complexes can be made with a wide variety of attached ligands, some of which are negatively charged, for example, $CI^-$, $CN^-$ and so on, and some of which are electrically neutral, for example, $H_2O$, $NH_3$, and so on. However, one thing that all ligands have in common is that they direct electrons – usually a lone pair – toward the metal ion, and these electrons become the 'point charges' in the crystal field model describing the electronic structure of the complex. Since the ability of different ligands to perturb the *d*-orbitals varies considerably, the spitting between the $t_{2g}$ and $e_g$ sets of orbitals can be quite different for different complexes. In order to address this, CF theory denotes the splitting between the $t_{2g}$ and $e_g$ sets as $\Delta_o$, which is the *crystal field splitting parameter*. The subscript 'o' in $\Delta_o$ indicates that a crystal field of octahedral symmetry is being addressed. If there are no attached ligands – that is, in the free ion case – there can be no crystal field and $\Delta_o$ is zero. Since the splitting between the levels is different for different metal complexes, $\Delta_o$, which carries units of energy usually expressed in wavenumbers ($cm^{-1}$), varies over a wide range. However, the relative displacement of the $t_{2g}$ and $e_g$ levels *in terms of* $\Delta_o$ from the center of gravity, $E_o$, is the same for all octahedral complexes with the $e_g$ level at 0.6 $\Delta_o$ and the $t_{2g}$ level at –0.4 $\Delta_o$. These values arise because (2 orbitals) × (0.6 $\Delta_o$) + (3 orbitals) × (−0.4 $\Delta_o$) ≡ 0, which satisfies the center of gravity rule. It should be evident that $E_o$ is the *average crystal field*.

### 1.2.2 Other Crystal Fields

Numerous anticancer drugs containing $Pt^{2+}$ have a square planar geometry in which four ligands at the corners of a square are bonded to the metal ion (Figure 1.1). The best way to generate the square planar crystal field splitting pattern for the *d*-orbitals is to first consider an intermediate field called the *tetragonal crystal field*. Suppose that the charge on each of the two point charges on the plus and minus z-axis of the octahedral crystal field is slightly reduced in magnitude relative to the other four charges in the plane; or, the equivalent situation, wherein the magnitude of the charges on the plus and minus z-axis remain unchanged but the charges are moved to a greater distance from the metal ion than the four charges in the plane. In this case, the electrostatic field on the z-axis is *less than* the field seen by the metal ion on the x- and y-axes of the system. As a consequence of this *asymmetry* or non-equivalence in the field, all orbitals with z-components – that is, $d_{xz}$, $d_{yz}$ and $d_{z^2}$ – will have their energies *lowered*; that is, they will become *more stable* in the applied field (Figure 1.5). Since $d_{z^2}$ is pointed directly at the weaker charges on the z-axis, it must experience greater stabilization – that is, more lowering – than $d_{xz}$, $d_{yz}$ which are directed away from the point charges. As a consequence of the center of gravity rule, if some levels go down in energy, others – that is, $d_{x^2-y^2}$ and $d_{xz}$ – must become *less stable* and their energies must be raised.

The limiting case of the tetragonal distortion is the *square planar geometry* in which the two charges on the z-axis have been reduced to zero; that is, there are only four charges in the plane of the system. The removal of the axial charges causes a significant stabilization in $d_{z^2}$, which moves downward in the energy diagram and passes below (becomes more

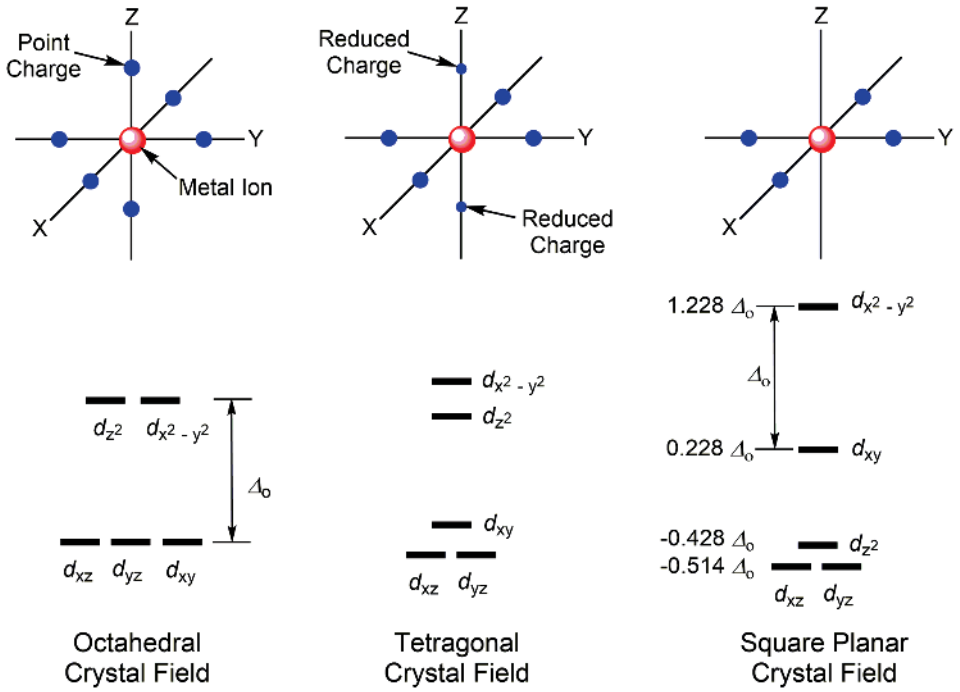


**Figure 1.5**
Octahedral, tetragonal and square planar crystal field.

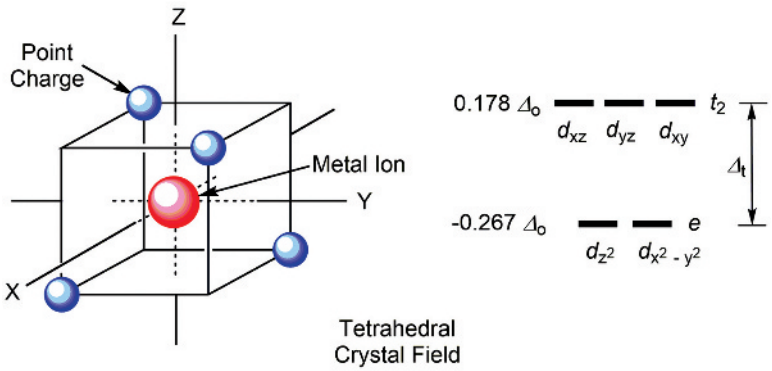


**Figure 1.6**
Tetrahedral crystal field.

stable than) the $d_{xy}$ orbital. Since $d_{xz}$, $d_{yz}$ also have z-components, they are also stabilized by the loss of the axial charges, but to a lesser extent than $d_{z^2}$. The resulting crystal field splitting diagram, sometime called the *square planar limit*, is shown in Figure 1.5.

A second very common structure for metal complexes with four groups bonded to the central metal ion is the *tetrahedral geometry* (Figure 1.1). Compared to the previous examples, rationalizing the *d*-orbital splitting pattern for the tetrahedral geometry is less straightforward. Figure 1.6 shows a Cartesian coordinate system in the center of a cube. Placement of charges at opposite corners of opposite faces of the cube and hypothetically connecting them to the metal ion in the center of the cube generates the tetrahedral geometry; that is, all charge–metal–charge angles are 109.5°. It should be evident from the figure that none of the *d*-orbitals point directly at the charges, and although other relative arrangements of the cube on the *d*-orbital coordinate system are possible, all lead to the conclusion given for the splitting pattern shown in Figure 1.6.

The tetrahedral crystal field has a doubly degenerate set of orbitals, the $d_{z^2}$ and $d_{x^2-y^2}$, termed for symmetry reasons the '*e*' set, which is *lowest* in energy, and a triply degenerate set, $d_{xz}$, $d_{yz}$ and $d_{xy}$, called the '$t_2$' set, which is *highest* in energy. While this pattern is exactly the opposite of the octahedral case, the labels *e* and $t_2$, which also come from group theory, are missing the subscript 'g'. This is because the octahedron has a symmetry element called the *center of inversion* (*i*), which is associated with a mathematical operation in which each point charge of the structure can be passed along a straight line through the central metal ion to reach an identical point charge (see Figure 1.5). Since *i* is not present in the tetrahedron, the subscript 'g' is missing from the labels. Although the tetrahedral pattern is the exact opposite of the splitting pattern for the octahedron, the magnitude of the splitting between the *e* and $t_2$ levels for the tetrahedral geometry, denoted as $\Delta_t$, is only 4/9 the value of the splitting between $t_{2g}$ and $e_g$ of the octahedron; that is, $\Delta_t = 4/9\ \Delta_o$ or $0.445\ \Delta_o$. Thus, for the tetrahedron, the $t_2$ orbital set is at $0.178\ \Delta_o$ and the *e* orbital set is at $-0.267\ \Delta_o$.

Table 1.1 gives the energies of the five *d*-orbitals for common geometries in terms of the octahedral crystal field splitting parameter, $\Delta_o$. The values in the table, which were calculated using a point charge crystal field model, can be used to determine the orbital energy diagrams for geometries other than the octahedral, tetrahedral, and square planar geometries discussed above. The entries in the table assume that if there is more than one electron in the pattern, which is almost always the case, there is no interaction between

**Table 1.1** Relative energies of the *d*-orbital in various crystal fields.[a]

| CN | Structure | $d_{z^2}$ | $d_{x^2-y^2}$ | $d_{XY}$ | $d_{Xz}$ | $d_{yz}$ |
|---|---|---|---|---|---|---|
| 2 | Linear[b] | 1.028 | −0.628 | −0.628 | 0.114 | 0.114 |
| 3 | Trigonal[c] | −0.321 | 0.546 | 0.546 | −0.386 | −0.386 |
| 4 | Tetrahedral | −0.267 | −0.267 | 0.178 | 0.178 | 0.178 |
| 4 | Square planar[c] | −0.428 | 1.228 | 0.228 | −0.514 | −0.514 |
| 5 | Trigonal bipyramid[d] | 0.707 | −0.082 | −0.082 | −0.272 | −0.272 |
| 5 | Square pyramid[d] | 0.086 | 0.914 | −0.086 | −0.457 | −0.457 |
| 6 | Octahedron | 0.600 | 0.600 | −0.400 | −0.400 | −0.400 |
| 7 | Pentagonal bipyramid[d] | 0.493 | 0.282 | 0.282 | −0.528 | −0.528 |
| 9 | Tricapped trigonal prism | −0.225 | −0.038 | −0.038 | 0.151 | 0.151 |

[a]Values given are in units of $\Delta_o$.
[b]Ligands or charges are along the z-axis.
[c]Ligands or charges are in the xy plane.
[d]Pyramid base in xy plane. From Table 9.14, p. 412 of Huheey, J.E. (1983) *Inorganic Chemistry: Principles of Structure and Reactivity*, 3rd edn, Harper & Row Publisher, New York.

the electrons, which is never the case. The energies given are the so-called *one-electron energies* for the various orbitals in the different crystal fields. If there is more than one electron in the pattern, the electrons can be in the same or different orbitals, and will 'see' each other through what are called *configuration interactions*, and the energies of levels given in Table 1.1 will be adjusted to new values. Since determining the new energies of the orbitals is beyond the scope of our work, and changes are in most cases small, the entries in Table 1.1 are reasonable approximations for all multiple-electron systems encountered in this text.

### 1.2.3 Factors Affecting the Crystal Field Splitting Parameter, Δ

#### *1.2.3.1 Spectrochemical Series*

As was earlier pointed out, the point charges used to generate the splitting patterns for various geometries simulate the electrostatic effects of ligands that are bonded to the metal ion. Extensive spectral and magnetic studies on a large number of transition-metal complexes showed that the electronic effect exerted by a specific ligand on the *d*-orbitals of the metal ion is essentially a property of that ligand and independent of the geometry of the complex, the nature of the metal ion, or its oxidation state. This characteristic allowed ranking of common ligands in terms of their '*d*-orbital splitting power,' to produce a series called the *spectrochemical series* (Table 1.2). Ligands on the left of the series, which are referred to as *weak field ligands*, for example $I^-$ and $Br^-$, cause a small splitting in the *d*-orbitals, while ligands on the right of the series, for example $CN^-$ (cyanide), CO (carbon monoxide) – *strong field ligands* – cause a large splitting in the orbitals. While there is little doubt that the order of the ligands in the series is correct (the order is obtained from experiment), the series does not seem to follow our intuitive feeling about which ligands should be high in the series and which should be low. For example, CO, which is uncharged, is highest in the series, but iodide, $I^-$, which is negatively charged, is lowest in the series. Based on the electrostatic arguments put forth in connection with the crystal field this makes little sense: $I^-$ should have a *greater* perturbation on the *d*-orbitals than uncharged CO. Clearly, factors other than simple electrostatic effects must influence $\Delta_o$. While the crystal field model

**Table 1.2** Factors affecting the crystal field splitting parameter, Δ

| | |
|---|---|
| The ligand[a] | *Spectrochemical Series, Increasing* Δ<br>$I^- < Br^- < S^{-2} < \underline{N}CS^- < Cl^- < \underline{N}O_3^- < N_3^- < F^- < OH^- < C_2O_4^{-2} \approx H_2O <$<br>$\underline{N}CS^- < CH_3C\underline{N} < \underline{N}H_3 <$ *en* $<$ *bipy* $<$ *phen* $< \underline{N}O_2^- < \underline{P}Ph_3 < \underline{C}N^- < \underline{C}O$ |
| The metal ion | *Principal Quantum Number, n*<br>First-row transition metal ion, 3*d* level, $\Delta^{3d}$<br>Second-row transition metal ion, 4*d* level, $\Delta^{4d} \sim 1.5\ \Delta^{3d}$<br>Third-row transition metal ion, 5*d* level, $\Delta^{5d} \sim 1.75\ \Delta^{3d}$ |
| The metal ion | *Oxidation State, Increasing* Δ<br>$M^+ < M^{2+} < M^{3+} < M^{4+} < M^{5+}$ |

[a]The underscored atom is the donor atom to the metal ion. *en*, ethylenediamine, 1,2- diaminoethane; *bipy*, 2,2′-bipyridine; *phen*, 1,10-phenanthroline.

works well for most of the cases encountered in this text, complexes which have considerable overlap between the orbitals on the metal and ligand – that is, when covalent bonding is present – cause the theory to 'bend' but not completely break down. How basic CF theory needs to be modified to accommodate this will be addressed in a later section.

#### *1.2.3.2 Principal Quantum Number, n*

While the spectrochemical series rank orders the experimentally measured effects of ligands on the splitting of the *d*-orbitals, it is also possible to make some general statements concerning the effects of the metal ion on the magnitude of Δ. If one moves down a given column in the Periodic Table, the quantum number *n*, which is called the *principal quantum number*, increases. For example, the first-row transition metal series elements have electrons in the 3*d* ($n = 3$) level, the second-row in the 4*d* ($n = 4$) level, and the third-row in the 5*d* ($n = 5$) level of the atom. Experimentally, it has been found that the magnitude of the crystal field splitting parameter Δ increases in the order $3d < 4d < 5d$, with $\Delta\ 4d \sim 1.5\ (\Delta\ 3d)$ and $\Delta\ 5d \sim (1.75\ \Delta\ 3d)$ (Table 1.2). The effects of this increase with *n* can easily be seen for the series $[Co(NH_3)_6]^{3+}$, $3d^6$, $[Rh(NH_3)_6]^{3+}$, $4d^6$ and $[Ir(NH_3)_6]^{3+}$, $5d^6$, which have identical geometries (octahedral), ligands (ammonia) and metal ion oxidation states (+3), and belong to the same family (column) of the Periodic Table. The values of $\Delta_o$ for these complexes are ∼22 000 $cm^{-1}$, ∼34 000 $cm^{-1}$ and ∼41 000 $cm^{-1}$, respectively, which shows that moving down a given column in the Periodic Table does indeed cause the values of the crystal field splitting parameter to *increase* by the approximate amounts given. Since atoms, and ions, become larger with atomic number, M–L bond lengths increase in moving from the first to the second and third rows of the transition metal series. Simple point-charge arguments would predict that if the M–L distance were increased, the magnitude of Δ would *decrease*, not increase as observed. The fact that the opposite is found is further proof that the simple point-charge model cannot be entirely correct, and that other factors are important in determining the magnitude of Δ.

#### *1.2.3.3 Metal Ion Oxidation State*

Experimentally, it can be shown that *increasing* the charge on the metal ion – that is, increasing its oxidation state – causes the *d-d* absorption bands of the complex to shift toward the ultraviolet (UV) region of the spectrum, which means that Δ has *increased* (Table 1.2).

Since the ionic radius of any ion decreases with an increase in the net positive charge on the ion, the *distance* between the metal ion and its bonded ligands must decrease when the oxidation state is increased. Since a decreased distance would lead to greater electrostatic repulsions between electrons on the metal ion and the ligands, the observed trends in $\Delta$ (with changes in oxidation state on the metal ion) *are* predicted by simple crystal field arguments.

### 1.2.4 High- and Low-Spin Complexes

When considering the ways in which electrons can occupy energy levels of an atom, ion or molecule, *Hund's rule* states that the electronic configuration with the lowest overall energy is one for which the spins for the electrons are unpaired, even if it means placing electrons in a nearby less-stable orbital (level) in order to do so. For the free ion, the five *d*-orbitals are degenerate in energy and electrons are added to the orbitals by *maximizing the number of unpaired spins*. If, for example, there are four electrons in the *d*-level of a free ion, it is possible to place the electrons in the level in a number of different ways, some of which are shown in Figure 1.7. Experimentally, Figure 1.7a, which has the maximum amount of spin unpairing, is known to be the lowest-energy (most stable) configuration. When describing the electron spin of any system, it is best to use the value of the magnetic spin quantum number, $m_s$, associated with the spin angular momentum of the electron. Each electron has spin angular momentum of $\pm{}^1/_2$ in units of $h/2\pi$. With $n$ electrons, the maximum possible value of the *total spin quantum number* $S$ is n/2 (all electrons unpaired) and the minimum possible value of $S$ is zero (if $n$ is even) or ${}^1/_2$ (if $n$ is odd). For simplicity, the term $h/2\pi$, where $h$ is Planck's constant, is usually dropped. Thus, for the configuration shown in Figure 1.7a, $S = (4)(1/2) = 2$, while $S$ for Figure 1.7b is $(+1/2 - 1/2 + 1/2 + 1/2) = 1$, and for Figure 1.7c is $(+1/2 - 1/2 + 1/2 - 1/2) = 0$. Two factors associated with electronic configurations – *coulombic interactions* and *spin correlations* – form the basis for Hund's rule. Since the placement of two electrons in the same orbital forces them to occupy the same regions of space, the coulombic repulsion between the electrons will be high, thus destabilizing the system. This obvious electrostatic repulsion makes it easy to see why maximum spin unpairing, maximum $S$, is desirable. While columbic considerations are important, the ability to exchange one electron with another in a given configuration *without changing S* is even more important. This aspect of Hund's rule, which is a product of quantum mechanics,

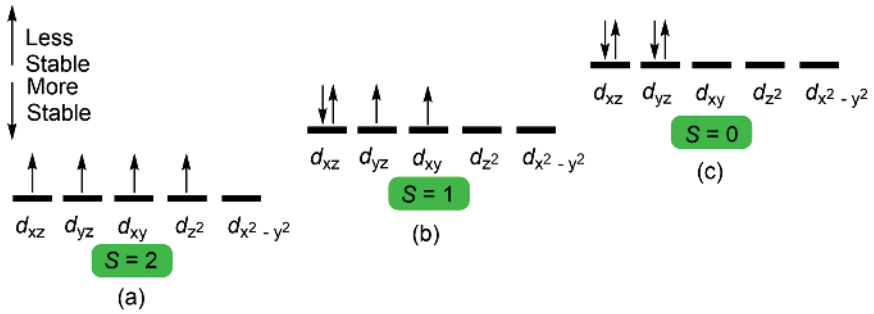


**Figure 1.7**
Some possible electronic configurations for the $d^4$ free ion and their respective values of $S$.

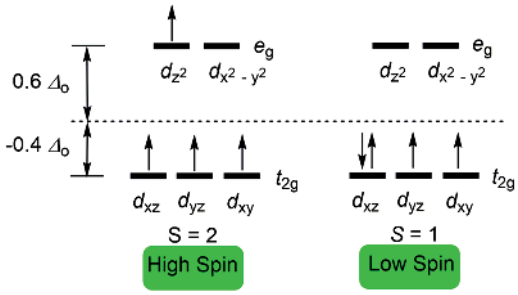


**Figure 1.8**
High- and low-spin possibilities for $d^4$ in an octahedral crystal field.

is called *spin correlation* or *exchange energy*. Both of these factors – coulombic (electrostatic) and spin correlation (exchange energy) – drive the system to obtain maximum spin unpairing, and for the free ion case, where all of the *d*-orbitals have the same energy, *the configuration with the largest value of S always has the lowest, most negative, energy*.

In the presence of an octahedral crystal field the five *d*-orbitals are not degenerate in energy, and a decision needs to be made on how to place the electrons into the *d*-orbital pattern to create the lowest energy configuration. For example, $d^4$ in an octahedral crystal field can have two possible electronic configurations, which are shown in Figure 1.8. One situation, called the *high-spin* case, has one electron in each of the three $t_{2g}$ orbitals and the fourth electron in one of the *d*-orbitals of the $e_g$ level, giving $S = 2$. The energy gained by the system due to the presence of the crystal field is called the *crystal field stabilization energy* (*CFSE*), which in this case is $\text{CFSE}_{\text{hs}} = (3 \text{ electrons})(-0.4\ \Delta_o) + (1 \text{ electron})(0.6\ \Delta_o) = -0.6\ \Delta_o$. This possibility can be written as $t_{2g}^3 e_g^1$. An alternative possibility for arranging the electrons in the levels is also shown in Figure 1.8. In this case, all four electrons are in the $t_{2g}$ set of orbitals and since *Pauli's principle* must be obeyed, two of the electrons in the same orbital must have their spin oppositely aligned. This gives $S = 1$ for the configuration, which is called the *low-spin case*. The crystal field crystallization energy for this configuration is $\text{CFSE}_{\text{ls}} = (4 \text{ electrons})(-0.4\ \Delta_o) = 1.6\ \Delta_o + P$, where $P$ is the energy required for pairing two of the electrons in one of the orbitals. This possibility can be written as $t_{2g}^4$. Since $P$ is the energy lost due to coulombic and exchange effects, its sign is *positive*, meaning that it *destabilizes* the system. Whichever possibility is found – high-spin or low-spin – clearly depends on which CFSE – $\text{CFSE}_{\text{ls}}$ or $\text{CFSE}_{\text{hs}}$ – has the larger *negative* value. This can be found by equating $\text{CFSE}_{\text{ls}}$ to $\text{CFSE}_{\text{hs}}$, which gives $1.6\ \Delta_o + P = -0.6\ \Delta_o$ or $P = \Delta_o$. If the ligands bonded to the metal ion produce a splitting in the *d*-orbitals with $\Delta_o > P$, the *low-spin* possibility, $S = 1$, will be more stable. If the ligands produce a splitting with $\Delta_o < P$, the *high-spin* situation, $S = 2$, will be more stable.

The electronic configuration, value of *S* and CFSE for weak and strong octahedral fields are given in Table 1.3. A point to make concerning the entries in Table 1.3 is that the value of CFSE given is the stabilization energy that the system accrues as a result of the presence of the directional crystal field. This means that the 'reference point' for determining the CFSE is the spherical field (Figure 1.4). For example, for the strong-field configuration, $t_{2g}^6$, which has $S = 0$, the value of CFSE in Table 1.3 of $-2.4\ \Delta_o + 2P$ was determined by first writing the electronic configuration for spherical field and determining its energy in terms of $P$, the pairing energy. With six *d*-electrons and five orbitals, there must be one

**Table 1.3** Crystal field effects for weak and strong octahedral fields.[a]

| Weak field (high-spin) | | | | Strong field (low-spin) | | | |
|---|---|---|---|---|---|---|---|
| $d^n$ | Config. | $S$ | CFSE | $d^n$ | Config. | $S$ | CFSE |
| $d^1$ | $t_{2g}^1$ | $^1/_2$ | $-0.4\ \Delta_o$ | $d^1$ | $t_{2g}^1$ | 1/2 | $-0.4\ \Delta_o$ |
| $d^2$ | $t_{2g}^2$ | 1 | $-0.8\ \Delta_o$ | $d^2$ | $t_{2g}^2$ | 1 | $-0.8\ \Delta_o$ |
| $d^3$ | $t_{2g}^3$ | 3/2 | $-1.2\ \Delta_o$ | $d^3$ | $t_{2g}^3$ | 3/2 | $-1.2\ \Delta_o$ |
| $d^4$ | $t_{2g}^3 e_g^1$ | 2 | $-0.6\ \Delta_o$ | $d^4$ | $t_{2g}^4$ | 1 | $-1.6\ \Delta_o + P$ |
| $d^5$ | $t_{2g}^3 e_g^2$ | 5/2 | $0\ \Delta_o$ | $d^5$ | $t_{2g}^5$ | 1/2 | $-2.0\ \Delta_o + 2P$ |
| $d^6$ | $t_{2g}^4 e_g^2$ | 2 | $-0.4\ \Delta_o$ | $d^6$ | $t_{2g}^6$ | 0 | $-2.4\ \Delta_o + 2P$ |
| $d^7$ | $t_{2g}^5 e_g^2$ | 3/2 | $-0.8\ \Delta_o$ | $d^7$ | $t_{2g}^6 e_g^1$ | 1/2 | $-1.8\ \Delta_o + P$ |
| $d^8$ | $t_{2g}^6 e_g^2$ | 1 | $-1.2\ \Delta_o$ | $d^8$ | $t_{2g}^6 e_g^2$ | 1 | $-1.2\ \Delta_o$ |
| $d^9$ | $t_{2g}^6 e_g^3$ | $^1/_2$ | $-0.6\ \Delta_o$ | $d^9$ | $t_{2g}^6 e_g^3$ | 1/2 | $-0.6\ \Delta_o$ |
| $d^{10}$ | $t_{2g}^6 e_g^4$ | 0 | $0\ \Delta_o$ | $d^{10}$ | $t_{2g}^6 e_g^4$ | 0 | $0\ \Delta_o$ |

[a]The entries in the table are based on the energies of the levels as if only one electron were present in the system. Placing more than one electron in the levels produces electron–electron interactions, which change the energies of the levels, but this has been neglected in the values given. From Table 9.3, p. 374 of Huheey, J.E. (1983) *Inorganic Chemistry: Principles of Structure and Reactivity*, 3rd edn, Harper & Row Publisher, New York.

paired set of electrons or one unit of $P$ for the spherical field case. Next, the energy of the system due to the presence of the crystal field, in terms of $\Delta_o$ and $P$, was written, which in this case is $-2.4\ \Delta_o + 3P$. There are three pairs of electrons in the $t_{2g}$ set of orbitals; hence $3P$, and the extra energy in terms of $\Delta_o$ due to the crystal field is $-2.4\ \Delta_o$. Taking the difference between the energy in the presence of the directional crystal field and the energy of the spherical field gives CFSE $= 2.4\ \Delta_o + 3P - P$ or $-2.4\ \Delta_o + 2P$. The remaining entries in Table 1.3 were calculated in a similar fashion. The values of CFSE for crystal fields of other symmetries can easily be obtained using the energies of the orbitals given in Table 1.1. As described above, the calculation of $S$ and CFSE assumes that there is no configuration interaction; that is, electrons in the pattern operate as independent non-interacting entities, in which case the one-electron energies in Table 1.1 can be used to estimate the energies of multiple electron cases.

## 1.3 Molecular Orbital Theory

The most important theory for discussing bonding in all of chemistry is molecular orbital (MO) theory. This theory uses the atomic orbitals (AOs) of all of the atoms in a compound to construct molecular orbitals (MOs), the shapes of which depend on the size and shape of, and distance between, atomic orbitals. A critical element of the theory is the wave function, denoted by $\psi$, which is a mathematical expression that when properly manipulated provides information on a physical system. If the wave function is associated with an atom, it can be used to calculate important properties of the atom, such as the probability of finding an electron in regions of space about the nucleus. If the wave function is associated with a molecule, it can be manipulated to provide information on the energies of bonds, the distribution of electrons in the molecule and other important quantities.

The wave function for an atom contains information on the *principal quantum number* ($n$), for example the '3' in 3*d*, the *orbital angular momentum quantum number* ($l$), for example the number associated with the letter '*d*' in 3*d*, and the *magnetic quantum number* ($m_l$), which distinguishes orbitals of a given $n$ and $l$. For a *d*-'subshell', $m_l$ has five values, which give rise to the five *d*-orbitals shown in Figure 1.2. For a *p*-subshell, $m_l$ has three values, which produce the three *p*-orbitals, $p_x$, $p_y$ and $p_z$, often discussed in organic chemistry. The fourth quantum number, called the *magnetic spin quantum number*, $m_s$, is associated with the spin angular momentum of the electron. As we have seen, it has values of +1/2 and −1/2 in units of $h/2\pi$, which refer to the spin moment of the electron relative to an electric or magnetic field. If two electrons occupy the same orbital, the values of $n$, $l$, and $m_l$ are the same but the spins of the electrons must be oppositely aligned; that is, $m_s$ for one electron must be +1/2 and $m_s$ for the second must be –1/2 $h/2\pi$.

### 1.3.1 MO Diagram of Molecular Hydrogen

The best way to describe MO theory at an elementary level is to show what happens when two hydrogen atoms ($H_A$ and $H_B$) come together to form a hydrogen molecule ($H_A$–$H_B$) (Figure 1.9). While molecular hydrogen has little relevance to metallo-drugs, qualitatively understanding how MO theory addresses the bonding in this simple molecule paves the way for understanding the bonding in more complicated metal complexes used in medicine.

MO theory starts with writing the complete (many-electron) wave function in terms of wave functions for individual electrons, and then each one-electron wave function is written in terms of atomic orbitals. The specific approach for molecular hydrogen is to carry out *linear combinations of atomic orbitals* (LCAO) by taking the sum and difference of the AOs on both hydrogen atoms to find new, *molecular*, wave functions that are associated

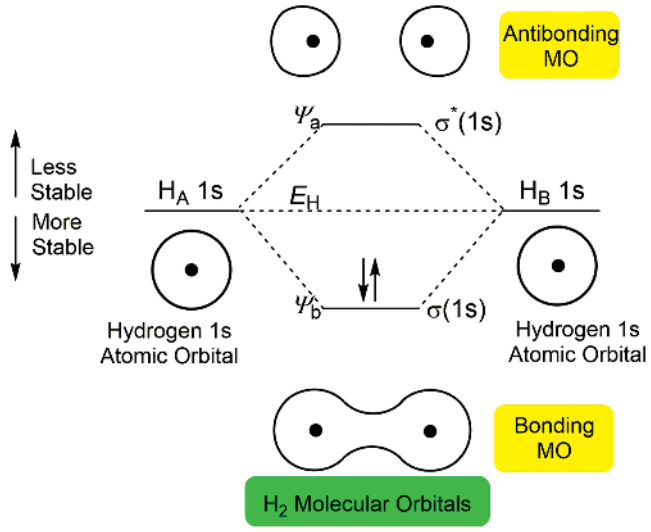


**Figure 1.9**
Molecular orbital diagram for molecular hydrogen, $H_2$. The black dots represent the hydrogen nucleus, a proton.

with the $H_2$ molecule. For molecular hydrogen, LCAO gives Eqs (1.1) and (1.2):

$$\Psi_b = [c_1\psi_A(1s) + c_2\psi_B(1s)] \quad (1.1)$$

$$\Psi_a = [c_1\psi_A(1s) - c_2\psi_B(1s)] \quad (1.2)$$

In these expressions, $\Psi_b$ is called the *bonding* molecular wave function and $\Psi_a$ the *antibonding* molecular wave function for the hydrogen molecule, while $\psi_A$ and $\psi_B$ are the atomic wave functions for the 1s orbitals on the two hydrogen atoms that were joined together to form the hydrogen molecule. The quantities, $c_1$ and $c_2$, which are positive, are simply weighting coefficients that determine the fraction (amount) of each atomic wave function to be used in making the molecular wave function. Conceptually, the expressions say that there are two ways to combine the 1s orbitals on the two hydrogen atoms, $H_A$ and $H_B$, when the hydrogen molecule is formed. One gives the bonding MO associated with the bonding wave function [Eq. (1.1)]. This MO gives a spatial volume that allows the electron to be found a significant fraction of the time between the two nuclei (Figure 1.9). The second way to do the combination gives the antibonding MO associated with the antibonding wave function [Eq. (1.2)]. This MO produces a shape that *prohibits* the electron from being found midway between the two nuclei (Figure 1.9). Both of these MOs are referred to as being *sigma type*; that is, they are associated with σ *bonds*, meaning that electron density for these MOs is on the bond axis of the system. In MO language, the bonding MO is labeled σ(1s), while the antibonding MO is denoted σ*(1s). For comparison, the other type of MO commonly encountered in chemistry is the *Pi type*, or simply π-*bond*, for which electron density is *not* on the bond axis of the system.

As shown in Figure 1.9, the energies of the 1s AO for both $H_A$ and $H_B$, $E_H$, must be identical because both atoms are identical. The energy of σ(1s) MO is lowered from $E_H$ and it becomes more stable than the σ*(1s) MO, which is raised in energy from $E_H$. For this situation in which the energies of the two AOs that formed the MOs are identical, the 'makeup' or composition of the σ(1s) MO and the σ*(1s) MO must have exactly equal contributions from both $\psi_A(1s)$ and $\psi_B(1s)$; that is, the coefficients $c_1$ and $c_2$ in Eqs (1.1) and (1.2) are the same and positive. This implies that electrons in this MO spend equal fractions of their time on either hydrogen atom of $H_2$. Once the molecular orbitals are formed and their approximate energies determined, the last step is to place the appropriate number of electrons into the diagram, filling the levels from bottom up, so that each MO holds two electrons with their spins oppositely aligned (Figure 1.9). Since each hydrogen atom brings one electron to the bonding scheme, the two electrons are placed in the lowest-energy MO, giving the electronic configuration for $H_2$ of $\sigma(1s)^2$, which is called the *ground state* of the hydrogen molecule. This stabilizes the hydrogen molecule relative to the two atoms and produces the well-known two-electron single covalent bond for molecular hydrogen. As is shown in Figure 1.9, the antibonding MO is not occupied by electrons when $H_2$ is in the ground state. However, it can be occupied by an electron if one of the electrons in the σ(1s) MO is moved to the σ*(1s) MO. This event, which would obviously require the addition of energy, is called an *electronic transition*, which could happen if $H_2$ were to absorb a photon with an energy equal to the energy spacing between σ(1s) and σ*(1s). The resulting electronic configuration, which is written as $\sigma(1s)^1\sigma^*(1s)^1$, is referred to an *excited state* of the hydrogen molecule, which when produced effectively eliminates the bond between the two hydrogen atoms; that is, one electron is in a bonding MO and one is in an antibonding MO. However, since the lifetime of the excited state is short, $\sim 10^{-9}$ s, dissociation of the hydrogen molecule into hydrogen atoms does not appreciably occur under conditions for which the transition can be observed. Located at higher energy (less stable) than the

1s atomic orbital is the 2s atomic orbital of hydrogen. These atomic orbitals interact with one another to produce another set of MOs, σ(2s) and σ*(2s), which, if $H_2$ is in the ground state, are at very high energy and are not occupied.

The basic features of the diagram shown in Figure 1.9 are the same as the features in the diagrams obtained from the application of CF theory. In an octahedral crystal field, a level, $e_g$, is raised in energy relative to some reference point, $E_o$, and a second level, $t_{2g}$, is lowered relative to $E_o$ (Figure 1.4). Placement of electrons in the lower level *stabilizes* the system, but adding electrons to the upper level *destabilizes* the system. While there are some similarities between the two theories, they are quite different in the way that they handle the role of the ligands in the bonding model. In CF theory the ligands are assumed to be point charges and their presence splits the *d*-orbitals into some pattern. The electrons that were originally on the metal ion before it was involved in complex formation are still 100% on the metal ion, and any electronic transitions that are possible can only take place within the split *d*-orbital set. MO theory, on the other hand, considers that all atomic orbitals on all atoms can potentially interact to produce new orbitals called *molecular orbitals*. The extent to which these interactions occur is determined by the shapes of the atomic orbitals and their energies, and the amount of each AO that is 'mixed into' the MO, which is in turn controlled by the weighting coefficients in expressions similar to Eqs (1.1) and (1.2). In reality, if all of the orbitals on all of the atoms are addressed in this manner, the mathematics and the subsequent electronic structure become very complicated. Fortunately, inorganic chemists have learned to focus on only those parts of a complete MO diagram that are most relevant to the property of the system being addressed.

### 1.3.2 MO Diagram for $[Co(NH_3)_6]^{3+}$

Consider the *partial* MO diagram for the octahedral complex, $[Co(NH_3)_6]^{3+}$, shown in Figure 1.10. While the complete diagram is more complicated than that given, Figure 1.10 contains enough detail to show how a diagram for a metal complex is created and what information it contains. The MO diagram is divided into three parts. The left side shows the relative energies of the 3*d*, 4*s* and 4*p* AOs on $Co^{3+}$, the right side gives the orbitals on the six ammonia molecules that interact with the orbitals on the metal ion, and the center shows the MOs that form from all of the AOs that are brought to the bonding scheme by the bonded partners. The orbitals on the right side of the diagram are actually the hybrid orbitals, $sp^3$, associated with the lone pair of electrons on the ammonia molecule. Since there are six ammonia molecules, there are six lone pairs, each having the same energy. While the fundamental 'units' used in MO theory are the atomic wave functions, 'mixing' some combination of AOs – for example, combining parts of the 2*s* orbital with the $2p_x$, $2p_y$, and $2p_z$ on nitrogen to form a 'hybrid' orbital – and entering the resulting hybrid orbital into the molecular orbital scheme produces the same mathematical result as using the unhybridized orbitals.

The dotted lines on the diagram show which metal and ligand AOs have been combined to form a particular MO. In order for atomic orbitals on M and L to combine and form a molecular orbital, the AOs on each must have shapes that allow the orbitals to overlap with one another. The labels used on the AOs (upper-case letters) and MOs (lower-case letters) are derived from *group theory*, which is branch of mathematics concerned with the symmetry properties of structures. In addition, the MOs indicate the type of orbital formed; in this case all are σ type. The MOs in the lower portion of the diagram are bonding MOs, while those in the upper part of the diagram, indicated with an asterisk, are antibonding MOs.

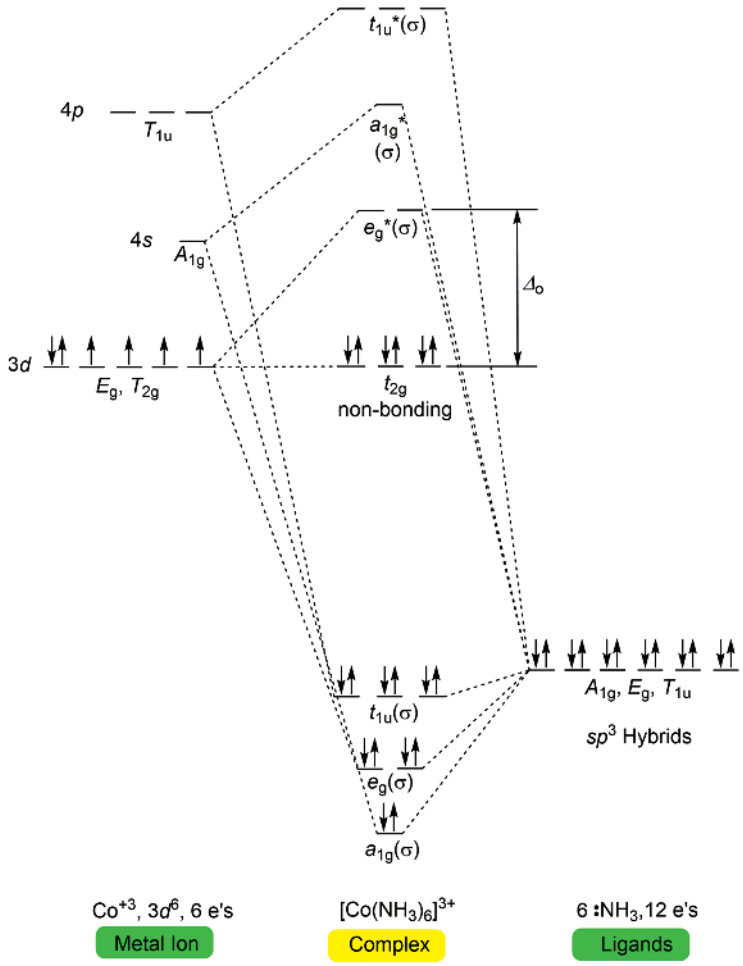


**Figure 1.10**
Molecular orbital diagram for $[Co(NH_3)_6]^{3+}$, σ bonding only.

The composition of a molecular orbital is determined by the relative energies of the atomic orbitals. If the energies of two interacting AOs are the same, as would occur with a homonuclear diatomic molecule like $H_2$, the values of $c_1$ and $c_2$ in Eqs (1.1) and (1.2) are the same. If the energies of the two interacting orbitals are not the same, as would occur when two different atoms are bonded to each other – that is, a heteronuclear diatomic molecule – and the AO on atom 'B' is more stable (at a lower negative energy) than the AO of atom 'A', $c_2$ is greater than $c_1$. For the opposite situation, where the energy of A > B, then $c_2$ is less than $c_1$. For transition metal complexes which contain many atoms there are often more than two AOs contributing to a particular MO, which means that the wave functions are much more complicated than Eqs (1.1) and (1.2). While it is not easy to determine how much each wave function contributes to these MOs – that is, the coefficients, $c_n$, in expanded versions of Eqs (1.1) and (1.2) – it is straightforward to determine which centers, metal ions or ligands, make the *major* contribution to the MO – that is, the largest value of $c_n$. For example, consider the bonding MO, $t_{1u}$ (σ), and its antibonding complement, $t_{1u}$

($\sigma^*$), shown in Figure 1.10. The fact that the energy of $t_{1u}$ ($\sigma$) lies closer to the energy of the ammonia atomic orbitals than any of the metal atomic orbitals in the diagram means that this MO contains *more* ligand character than metal character; that is, the weighting coefficients, $c_n$, for the wave functions from L are greater than the coefficients for the wave functions associated with M. Conversely, $t_{1u}$ ($\sigma^*$), which is close in energy to AOs on the metal ion – for example 4*p* – must have contributions that are weighted heavily in favor of the AOs on the metal ion. All of this means that $t_{1u}$ (s) is mostly ligand in character and its complement, $t_{1u}$ ($\sigma^*$), is *mostly metal in character*. With one exception, all of the MOs in the diagram are compositions of AOs from both L and M, with $a_{1g}$ ($\sigma$), $e_g(\sigma)$ and $t_{1u}(\sigma)$ being mostly ligand in character and $e_g(\sigma^*)$, $a_{1g}(\sigma^*)$, $t_{1u}(\sigma^*)$ being mostly metal in character. The $t_{2g}$ set of *d*-orbitals, which are directed off the axes of the system, have no orbitals with which they can interact on the ammonia side of the diagram. The reason for this is not so easy to explain, but is related to the fact that none of the symmetry properties of the orbitals that are coming from the ligands on the right side of the diagram match the symmetry properties of the $t_{2g}$ set from the metal ion on the left side of the diagram. One of the requirements for the formation of an MO is that the symmetries of the interacting AOs must match, and there must be no $T_{2g}$ term on the right side of the diagram. Without any interacting orbital on the ligand side of the diagram, members of the $t_{2g}$ set appear in the diagram as 'pure' *d*-orbitals and as such are not really molecular orbitals at all. In the MO description of the bonding, they are referred to as *nonbonding* orbitals. For certain ligands, for example $CN^-$ and CO, there are antibonding $\pi$-type MOs on the *ligand* that can interact with the $t_{2g}$ set on the metal. In this situation, the $t_{2g}$ set can form a $\pi$-bond between M and the carbon atoms on the ligands, which results in bonding and antibonding $\pi$-type MOs in the MO diagram.

## Box 1.1 Organometallic Chemistry

Organometallic chemistry is a broad area of science that studies the structures and properties of compounds with metal–carbon bonds. A characteristic feature of organometallic compounds, which distinguishes them from coordination complexes, is that their bonding is largely covalent in nature. Consider the MO diagrams for the organometallic compound $Cr(CO)_6$, hexacarbonylchromium (Figure 1.11), and the coordination compound $[Co(NH_3)_6]^{3+}$ (Figure 1.10).

Inspection of these diagrams shows that while the atomic orbitals, AOs, on the metal sides for $Co^{3+}$ and $Cr^0$ are the same – the 3*d*, 4*s* and 4*p* are used in the MO bonding scheme – the right, ligand, sides are very different between the two compounds. For $[Co(NH_3)_6]^{3+}$ there are six hybrid $sp^3$ orbitals from the six ammonia molecules on the right side, while for $Cr(CO)_6$ there are six $\sigma$-orbitals and twelve $\pi^*$-orbitals from the six CO molecules on the ligand side of the diagram. The boundary surfaces – that is, where the electrons are found – for the $\sigma$ (2p) and one of the $\pi^*$ (2p) MOs on carbon monoxide, and the way in which these MOs interact with two of the AOs on the metal to form a metal–carbonyl bond, are shown in Figure 1.12. As is evident from Figure 1.12, the $\sigma$ MO of CO interacts with the AO of Cr to form a $\sigma$-type bond between the carbon atom of CO and Cr, which produces the bonding, $e_g(\sigma)$, and antibonding, $e_g^*(\sigma)$, molecular orbitals for $Cr(CO)_6$, shown in Figure 1.11. While this Cr–CO $\sigma$-bond is similar to the $\sigma$-bond between the $Co^{3+}$ ion and the lone pair

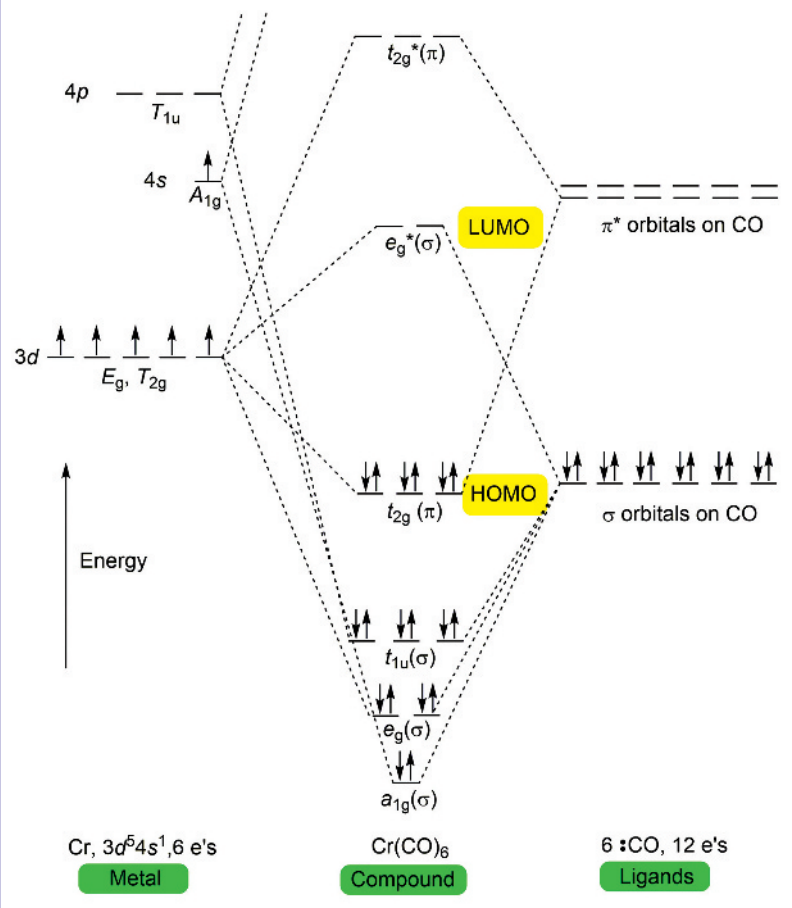


**Figure 1.11**

Partial molecular orbital diagram for $Cr(CO)_6$. The energies of levels are only approximate. Antibonding MOs at high energy (less stable) are not shown in the diagram. While there are a total of 12 $\pi^*$ MOs on the six carbon monoxide molecules, for reasons pertaining to symmetry, only three $\pi^*$ MOs on the COs are used in interacting with the $t_{2g}$ orbitals ($d_{xz}$, $d_{yz}$, $d_{xy}$) on the metal to produce bonding, $t_{2g}$, and antibonding, $t_{2g}^*$, MOs. The lowest unoccupied molecular orbital, LUMO, and highest occupied, HOMO, are also shown on the diagram.

of electrons in the $sp^3$ hybrid of $NH_3$ of $[Co(NH_3)_6]^{3+}$ (Figure 1.10), the fact that the energy of the σ MOs of CO is near the energy of the 3*d* orbitals on the metal means that the wavefunctions for the $e_g(\sigma)$ bonding and $e_g^*(\sigma)$ antibonding MOs for $Cr(CO)_6$ have significant contributions from the atomic wavefunctions of both M and L through expressions like Eqs (1.1) and (1.2). In simple terms, this means that electrons in these MOs for $Cr(CO)_6$ (there are four electrons in $e_g(\sigma)$) do not belong to either Cr or CO but rather are shared by both bonding partners; that is, the bond is *covalent*. This situation is different from that of $[Co(NH_3)_6]^{3+}$, for which the energies of the ammonia hybrids are much lower (more stable) relative to the 3*d* orbital of the metal, which make the wavefunction for the $e_g$ (σ) bonding MO heavily weighted in favor

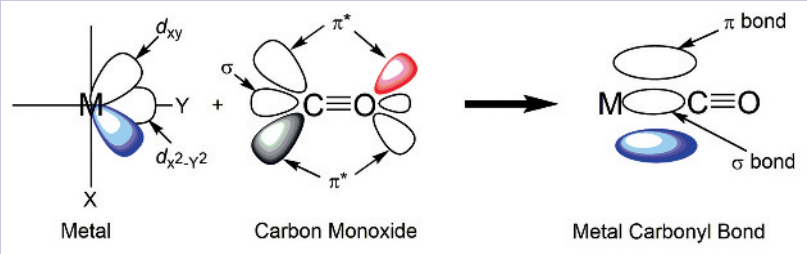


**Figure 1.12**

Bonding between carbon monoxide and a metal to form a metal carbonyl bond. For clarity, only portions of the $d_{x^2-y^2}$ and $d_{xy}$ orbitals on the metal are shown. The metal carbonyl bond is formed using the σ (2p) MO on CO and the $d_{x^2-y^2}$ atomic orbital on M, while the π-bond between M and CO is formed using a π* (2p) MO on CO and the $d_{xy}$ atomic orbital on M. The shaded and unshaded orbitals indicate that the sign of the wavefunction is positive and negative, respectively.

of the AOs of the ammonia hybrids. This shows that the four electrons in the $e_g(\sigma)$ bonding MO of $[Co(NH_3)_6]^{3+}$ spend more time on the ammonia molecules than on the cobalt ion, and the bond between ammonia and the metal ion is ionic or salt-like in nature. This change in the nature of the bonding from ionic to covalent means that in the latter case it is not possible to clearly assign oxidation state; that is, electrons in the bond spend significant fractions of their time on both M and L, and oxidation state is often assigned using a simple 'book-keeping' procedure, with the value obtained referred to as the formal oxidation state.

Another important difference between the MO diagrams for $[Co(NH_3)_6]^{3+}$ and $Cr(CO)_6$ is that the $t_{2g}$ set of orbitals in Figure 1.10, which had no orbitals on ammonia with which to interact and were labeled 'nonbonding', now interact with the π* MOs on CO in the manner shown in Figure 1.11. This interaction produces a bonding MO, $t_{2g}$ (π), which is lowered in energy relative to its contributing AOs, and an antibonding MO, $t_{2g}{}^*(\pi)$, which is raised in energy relative to its contributing AOs. As shown in Figure 1.12, this interaction results in a π-bond between the metal and the carbon atom of CO. Since the orbitals of the bonding partners bring a total of 18 electrons to the bonding scheme, and the electrons are placed into the MOs of $Cr(CO)_6$, filling from the bottom up, the highest occupied molecular orbital (HOMO) is $t_{2g}(\pi)$ and the lowest unoccupied molecular orbital (LUMO) is $t_{2g}{}^*(\pi)$. A transition metal can only contribute nine atomic orbitals to the bonding scheme shown in Figure 1.11 – that is, nd, (n + 1)s and (n + 1)p – which will, if there are σ and π MOs, interact with nine orbitals on the ligands to produce 18 MOs. Nine of these MOs are bonding MOs, which when occupied by electrons stabilize the system, and nine are antibonding, which when occupied by electrons destabilize the system. If the ligand is a good σ-donor and π-acceptor (as is the case with CO) and many arene-type ligands, the energy gap between HOMO and LUMO in Figure 1.11 is large, which has important consequences for the overall stability of the compound. For compounds contributing more than 18 electrons to the bonding diagram, as will occur if the nature of the transition metal or the ligands is changed, one or more electron(s) will be forced to occupy antibonding MOs in the diagram, which will lower the stability of the compound. For compounds contributing fewer than 18 electrons, not all of the possible bonding MOs

will be occupied, which will also lead to a decrease in the stability of the system. Thus, the 18 electrons in the diagram produce a compound with the maximum stability, which is the basis for the effective atomic number rule or 18-electron rule in organometallic chemistry. If a metal has an odd number of electrons in its valence shell, for example manganese, Mn, $3d^5 4s^2$, it will not be possible to achieve the even number of 18 electrons. In this case, the carbonyl compound with maximum stability is bis(pentacarbonymanganese), $Mn_2(CO)_{10}$, which has an Mn–Mn bond. Since the two electrons in the metal–metal bond are shared between both Mn atoms, at least some of the time an additional electron from the adjacent Mn atom can be added to the 17 electrons of each $Mn(CO)_5$ unit, allowing the compound to obey the 18-electron rule.

Aside from CO, nitric oxide (NO), and other small molecules, there is a wide variety of unsaturated arene-type organic compounds that are good σ-donors and π-acceptors and that can react with transition metals to form organometallic compounds. One famous example is ferrocene, the synthesis of which is shown in Figure 1.13. Ferrocene can be made by treating cyclopentadiene with sodium hydroxide or another suitable base, which removes the acidic hydrogen of the diene to form the aromatic cyclopentadienyl ion, Cp. Reaction of two Cps with ferrous chloride produces the 'sandwich' compound ferrocene, $(\eta^5\text{-}C_5H_5)_2Fe$ ($FeCp_2$), which has two Cp ligands face-on-bonded to the iron ion. The nomenclature used to indicate the number of points of attachment of the arene ligand to the metal is the Greek letter η (eta), which carries as a superscript the number of ligand attachment points, which in this case is 5, for the five carbon atoms of Cp.

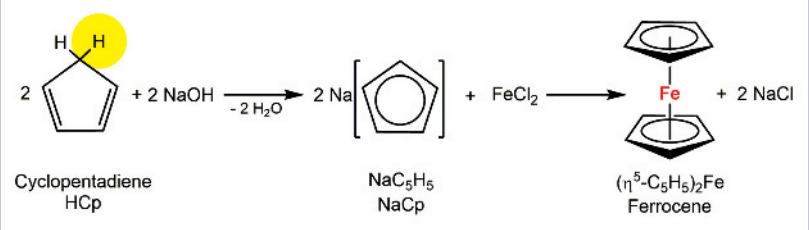


**Figure 1.13**
Synthesis of ferrocene.

Ferrocene, which is very stable, obeys the 18-electron rule. Brought to the bonding scheme for ferrocene are 12 electrons from the two Cp ligands (each Cp is a six-electron donor; four π-electrons plus the two electrons in the negative charge) and six electrons from the valence shell of the $Fe^{2+}$ ion, $3d^6$. Since the 18 electrons are in MOs that have significant contributions from both M and L, the concept of the formal oxidation state is applied when determining the oxidation of the iron in ferrocene. If the Cps are negatively charged and six-electron donors, the iron has a formal oxidation state of $Fe^{2+}$, but if the two Cps are uncharged and five-electron donors, the formal oxidation state of the iron is $Fe^0$. As will be apparent, benzene, $C_6H_6$, and its analogs can also form sandwich-type organometallic compounds. In this case, the benzene ring is considered as contributing six electrons (the electrons in three π-bonds) to the bonding scheme.

It should be evident that determining even the approximate composition of MOs depends critically on the relative energies of the metal and ligand orbitals. The property of the orbital that approximates its relative energy in an MO diagram is its *electronegativity*, and the hybrid orbital of the ammonia molecule is more electronegative (has greater negative energy) than are the 3*d* atomic orbitals of $Co^{3+}$. If the reverse were true – that is, if the energies of the ligands were raised, less stable, relative to the metal orbitals – the positions of the MOs would be shifted upward in the diagram and compositions of the resulting MOs, in terms of their contributing AOs, would be the reverse of those described above and shown in Figure 1.10

A final point to make in connection with the MO diagram is the appearance of the molecular orbitals. Consider $a_{1g}(\sigma)$, which is the most stable bonding MO in Figure 1.10. The wave function for this MO would have contributions from the six $sp^3$ hybrids on the ammonia molecules, with each hybrid being a combination of the 2*s* and 2*p* orbitals on nitrogen, and the 4*s* orbital on the metal ion. When this molecular wave function is used to calculate the boundary surface for the MO, a structure similar to that given in Figure 1.14 results, confirming that electrons in $a_{1g}(\sigma)$ would more likely be found on the ligands than on the metal ion. It should be evident that MOs for multi-atom systems are quite complex, and for the purposes of the brief overview of MO theory given here it is more important to understand the location, electron occupancy and approximate composition of an MO rather than its detailed shape.

The procedure for placing electrons into the diagram is to fill the diagram, from the bottom to the top, with the total number of electrons that were originally in the orbitals on M and L that created the diagram. In this case there are six electrons from the $Co^{3+}$ ion and 12 electrons from the six lone pairs on the ammonia molecules. Since each individual MO can only hold two electrons with their spins oppositely aligned, the occupancy of the MOs for the *ground state* of the system is that shown in Figure 1.10. A critical feature of the diagram is that the central portion of the MO diagram is exactly the splitting pattern predicted by CF theory. There is a triply degenerate set, $t_{2g}$, which is *nonbonding* in the MO diagram, that is separated from a doubly degenerate set at higher energy, which is the antibonding MO, $e_g^*$. Calculations show that the distance between these levels is $\Delta_o$, as indicated on the diagram. A photon with the correct energy entering the system could cause one of the electrons in the $t_{2g}$ set to be promoted to a vacant level in the $e_g^*$ set which, aside

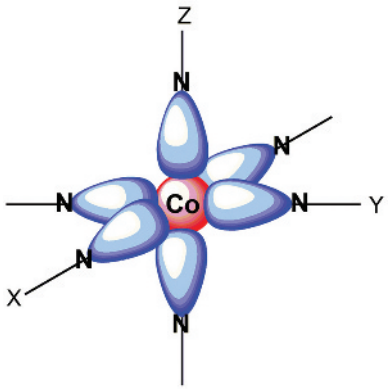


**Figure 1.14**
Approximate shape of the $a_{1g}$ ($\sigma$) bonding molecular orbital for $[Co(NH_3)_6]^{3+}$.

from the slight change in the labels of the levels, is exactly what is predicted by CF theory. However, unlike CF theory, MO theory provides a much more comprehensive picture of bonding in that transitions outside the *d*-level of the metal ion are possible. For example, since the composition of an MO depends on the amount and types of AOs that created it, an electron in an excitation process could start out from an MO that is mainly ligand in character, for example $t_{1u}$ ($\sigma$), and end up in an MO which is mainly metal in character. This type of transition, which cannot be accommodated by simple CF theory, is called a *charge transfer transition*, in which charge is transferred from the ligand to the metal ion during the absorption process. Since the direction of the charge transfer is from L to M, the transition carries the acronym *LMCT*, for *ligand-to-metal charge transfer*. While the diagram in Figure 1.10 does not have this as a possibility, an electron could also start out in an MO that is mainly metal in composition and terminate in an MO that is mostly ligand in character. Such a transition carries the acronym *MLCT*, for *metal-to-ligand charge transfer*.

While there is no doubt that MO theory is the most comprehensive way to analyze bonding in chemistry, it requires many parameters and even in its qualitative form is quite challenging. Fortunately, CF theory along with a basic knowledge of MO theory will suffice to understand the physical and chemical properties of most of the metal complexes encountered in this text.

## 1.4 Absorption Spectra of Metal Complexes

One of the most striking characteristics of transition metal complexes is that they are brightly colored. Once it was learned that the absorption bands giving rise to the color were associated with electronic transitions mainly within the *d*-level of the ion, efforts were made to understand the origin of the bands in terms of the electronic structure of the compounds using crystal field theory. Shown in Figure 1.15 is the absorption spectrum of $[Ti(H_2O)_6]^{3+}$,

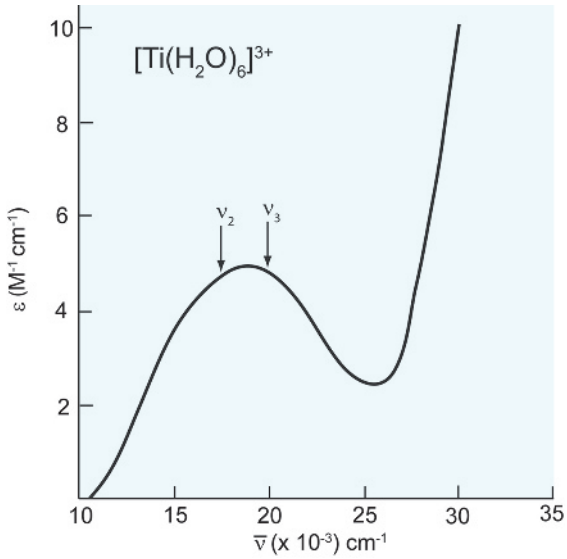


**Figure 1.15**
Absorption spectrum of $[Ti(H_2O)_6]^{3+}$ in water. Adapted from Lever, A.B.P., *Inorganic Electronic Spectroscopy*, 1968, Elsevier. Reproduced with permission of Elsevier.

$3d^1$, a metal complex that is purple in color. This complex is an octahedral structure with the single *d*-electron on the $Ti^{3+}$ ion in the lower triply degenerate set of *d*-orbitals; that is, the electronic configuration is, $t_{2g}^1 e_g^0$ (Figure 1.4). Since there is a higher-energy unoccupied level, $e_g$, it is possible to promote the electron in the lower level to the higher level if the wavelength of light falling on the sample is of the correct energy to bridge the energy gap, $\Delta_o$, between $t_{2g}$ and $e_g$. Thus, simple CF theory predicts that $[Ti(H_2O)_6]^{3+}$ should have a single electronic transition, designated as $t_{2g}^1 e_g^1 \leftarrow t_{2g}^1 e_g^0$, which should be equal to the crystal field splitting parameter, $\Delta_o$. Note that the spectroscopist writes this transition by listing the excited state first and having the transition arrow point to the excited state from the ground state, which is listed last.

## Box 1.2 Absorption Spectra of Metal Complexes

A UV–visible spectrophotometer is used to measure the absorption spectrum of a complex in solution. The instrument consists of a light source which emits many different wavelengths of radiation, a grating which systematically selects wavelengths to be passed through the sample, and a detector which measures the amount of radiation passing through the sample. If the solute in the solution absorbs light in a certain region of the spectrum, the photons which fall on the sample in this region will be reduced in number relative to the corresponding case in which only solvent is present in the light beam. While the absorbed radiation is quickly re-emitted by the solute, the emitted photons are distributed in all possible directions in space, causing the detector to 'see' fewer photons than were directed at the sample.

Each chemical compound has a characteristic absorption spectrum that shows how the compound absorbs light as a function of wavelength. The absorption of radiation by the sample is given by the Beer–Lambert law, $A = \log I_o/I_t = \varepsilon cl$ [1]. In this law, the absorbance or optical density, *A*, is the logarithm of the ratio of the intensity of radiation falling on the sample, $I_o$, to the intensity of radiation exiting the sample, $I_t$. The absorbance is also equal to the product of $\varepsilon$, the molar extinction coefficient (molar absorbtivity), *c*, the concentration of the solute, and *l*, the path length of the beam passing through the sample. If the unit of *c* is moles/liter (M) and the unit of *l* is centimeters (cm), the unit of $\varepsilon$ is $M^{-1}$ $cm^{-1}$, showing that the absorbance, *A*, is a *unitless quantity*. Each absorption band in a chemical compound has a characteristic value of $\varepsilon$, which is in effect a measurement of the 'photon-absorbing power' of that band. Since an absorption band is caused by a transition between states (levels) within the electronic structure of the compound, the magnitude of $\varepsilon$ is a measure of the 'allowedness' of the transition between the states. The value of $\varepsilon$, which varies over many orders of magnitude, allows the spectroscopist to assign the transition in terms of a specified set of *selection rules*.

There are a number of ways to display the absorption spectrum of a compound. The x-axis of the plot can be in *wavelength*, $\lambda$ (usually in nm, $10^{-9}$ m), but the spectroscopist prefers *wavenumber*, $\bar{\nu}$ (usually in $cm^{-1}$), where $\bar{\nu} = 1/\lambda$. The latter is used because the distance between states (levels) in the energy-level diagram of a compound is in units of energy, and since $E = h\nu$ and $\nu = c/\lambda$, energy, *E*, is proportional to $1/\lambda$, not $\lambda$. The y-axis of the plot is usually given in $\varepsilon$ (in units of $M^{-1}$ $cm^{-1}$). Sometimes, if the values of $\varepsilon$ span a large range, log $\varepsilon$ will be given or the units will

be in m$M^{-1}$ cm$^{-1}$, where m$M$ is $M$ multiplied by $10^{-3}$. Yet another variation is to multiply the actual value of $\varepsilon$ by some factor, for example $10^{-3}$, in order to reduce the number of 'zeros' that need to be given on the y-axis of the plot. Thus, if the actual value of $\varepsilon$ is 3000 $M^{-1}$ cm$^{-1}$, the label on the y-axis may be 3.0 $M^{-1}$ cm$^{-1}$, and indicate that the values shown should be multiplied by $10^3$ in order to obtain the actual value of $\varepsilon$. If absorbance, $A$, is given on the y-axis, one cannot determine the values of $\varepsilon$ unless $c$, the concentration, and $l$, the path length, are also given. In this case, the values of $\varepsilon$ must be calculated using the Beer–Lambert law.

A careful look at the spectrum in Figure 1.15 shows that the spectrum of $[Ti(H_2O)_6]^{3+}$ is a bit more complicated than expected: the absorption band is slightly broadened to its low-energy side. In fact, $[Ti(H_2O)_6]^{3+}$ experiences what is called a *Jahn–Teller distortion*, in which two of the water molecules that are *trans* to each other move slightly closer to the metal ion than the remaining four. This of course slightly changes the symmetry of the crystal field away from 'pure' octahedral to a *tetragonal* distortion of a kind similar to that described in connection with the generation of the square-planar crystal field (Figure 1.5). However, in this case the two ligands (charges) on the z-axis move closer to rather than farther away from the metal ion.

The Jahn–Teller effect applies to all chemical systems that have more than one way to indicate an electronic configuration. In this case, the single electron could be placed in any one of the three orbitals of the $t_{2g}$ set – that is, $d^1_{xz}$, $d_{yz}$, $d_{xy}$ or $d_{xz}$, $d^1_{yz}$, $d_{xy}$ or $d_{xz}$, $d_{yz}$, $d^1_{xy}$ – and all would yield the same CFSE and total energy. This situation is called a *triple orbital degeneracy,* and the Jahn–Teller theorem states that *the system must structurally distort in some way to remove the degeneracy and lower the overall energy of the system*. If the two water molecules on the z-axis are slightly 'pushed in' toward the metal ion relative to the remaining four in the plane, the octahedral splitting pattern would distort to the one shown in Figure 1.16, which has the $d_{xy}$ orbital at a lower energy (more stable) than $d_{xz}$

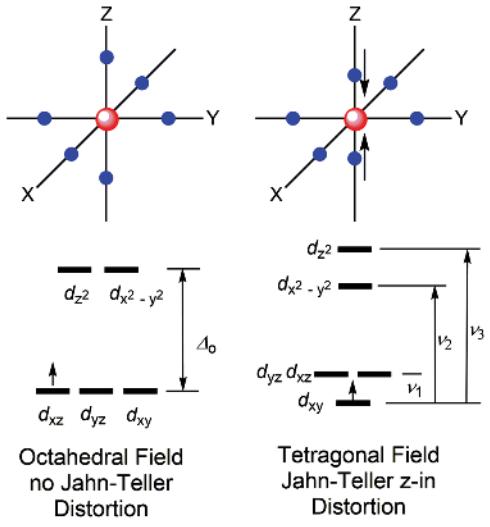


**Figure 1.16**
Jahn–Teller (tetragonal) distortion, '$z$-in', for $[Ti(H_2O)_6]^{3+}$, $3d^1$.

and $d_{yz}$ orbitals. This is called a '*z*-in' *tetragonal* Jahn–Teller distortion, because the two ligands on the z-axis of the system have been moved closer to the metal ion than the four in the plane. Of course, any structural change of this type would affect the $e_g$ set, causing the $d_{x^2-y^2}$ and $d_{z^2}$ to shift to new positions in the manner shown in Figure 1.16. Since the single electron must occupy the lowest orbital when the system is in the ground state of, for example, $d^1_{xy}$, there are now *three* transitions possible $-d_{xz}, d_{yz} \leftarrow d_{xy}$, $v_1$; $d_{x^2-y^2} \leftarrow d_{xy}$, $v_2$; $d_{z^2} \leftarrow d_{xy}$, $v_3-$ whereas there was only one – $t^0_{2g}e^1_g \leftarrow t^1_{2g}e^0_g$ – in the pure octahedral crystal field. It should now be clear that the hidden band to the low-energy side of the main band at ~17 400 $cm^{-1}$ in the spectrum of $[Ti(H_2O)_6]^{3+}$ is actually $v_2$, while the main band at ~20 100 $cm^{-1}$ is $v_3$ [2]. The lowest energy transition, $v_1$, which is quite small in energy, is in the infrared region of the spectrum and is not easily observed. From the above presentation it is clear that CF theory works well in explaining the absorption spectrum of $[Ti(H_2O)_6]^{3+}$, even accounting for a distortion in the structure of the complex due to the Jahn–Teller effect.

### 1.4.1 Band Intensity/Selection Rules

Quantum mechanically, all transitions between electronic states (levels) of chemical compounds are controlled by *selection rules*, which cause some transitions to be strong and others to be weak. For the kinds of compounds to be discussed in this text, two types of selection rule are important: one that pertains to the orbital motion of the electron, associated with the *orbital angular quantum number, l*; and a second associated with the spin of the electron specified by the *magnetic spin quantum number*, $m_s$. For an example of how the selection rule associated with orbital angular momentum works, consider the absorption band associated with the transition, $d_{x^2-y^2} \leftarrow d_{xy}$, $v_2$, for $[Ti(H_2O)_6]^{3+}$, which has the electron moving between two different *d*-orbitals. Since the electron starts out in a *d*-orbital, $d_{xy}$, which has $l = 2$, and it ends up in another *d*-orbital, $d_{x^2-y^2}$, which also has $l = 2$, the value of $l$ does not change in the transition; that is, $\Delta l = 0$. In this case the transition is forbidden by the *Laporte selection rule*, or to put it another way, the transition is *Laporte-forbidden*. The word 'forbidden' does not imply that the transition is totally absent – it is clearly visible in the spectrum shown in Figure 1.15 – but rather, it simply means that the transition has some restrictions on it that make it weaker (less likely to occur) than other possible types of transitions. If the quantum number $l$ changes in a transition – that is, $\Delta l \neq 0$ – the transition is said to be *Laporte-allowed* and the absorption band in this case would be much stronger (more likely to occur) than if $\Delta l \neq 0$. In discussing the bonding in $[Co(NH_3)_6]^{3+}$ using MO theory (Figure 1.10), it was pointed out that an electron located in an MO that was mainly *p* in character (strong ligand contribution) could move to an MO that was mainly *d* in character (strong metal contribution). An example of such a transition is the LMCT transition, $e^*_g \leftarrow a_{1g}$ (Figure 1.10), in which the electron starts out in an MO that is mainly ligand in character, $a_{1g}$, and terminates in an MO, $e^*_g$, that is mainly metal in character. Since $\Delta l \neq 0$ – that is, $d \leftarrow$ p – this transition is Laporte-allowed and its intensity is much greater than a transition with $\Delta l = 0$. While the MO diagram shown in Figure 1.10 does not have MLCT as a possibility (for example, $p \leftarrow d$), such a transition would also have $\Delta l \neq 0$, would be Laporte-allowed, and would be strong in intensity.

As will soon be evident, the net spin, *S*, can also change in an electronic transition. This happens when the net spin associated with the starting configuration (ground state) is different from the net spin of the ending configuration (excited state). The *spin selection rule*

addresses what happens to the spin during a transition; that is, it indicates the difference between the spins of the excited and ground states of the system, referred to as $\Delta S$. If $\Delta S = 0$, the transition is said to be *spin-allowed* and the net spin of the system is unchanged in the transition. If $\Delta S \neq 0$, the transition is said to be *spin-forbidden* and the net spin of the system must change in the transition. Experimentally, transitions that have $\Delta S = 0$ are much stronger (have a higher probability of occurring) than transitions that have $\Delta S \neq 0$. A simple explanation of why spin-forbidden transitions are weaker than their spin-allowed counterparts is related to the fact that a spin-forbidden transition requires two events to take place: one is the promotion of the electron to a higher energy level, and the other is a change in the spin of the electron during the promotion. This two-event situation is much less probable than the one-event situation of simply promoting the electron to another level without changing its spin.

A final comment on the intensity of absorption bands observed for transition metal complexes pertains to the symmetry of the complex. Mathematicians recognize that all objects in Nature have certain symmetry properties called *symmetry elements* that allow them to be systematically classified into a *point group*, which specifies a certain set of symmetry elements. Although the details of how this is done will not be given here, one symmetry element called the *center of inversion*, which is given the symbol *i*, is an important determinant of the intensity of a band in the absorption spectrum of a transition metal complex. Consider the structures of the tetrahedral and octahedral complexes shown in Figure 1.1, and note that for the octahedral arrangement of ligands the complex has a special point (the metal ion) through which each of the six ligands can be passed to reach an equivalent point: that is, another identical ligand. Carrying out this symmetry operation on the complex, passing all ligands through the center, will result in a structure which looks identical to the starting complex; that is, it will appear as if nothing was done to the complex. When this condition is met, the object is said to possess the center of inversion, *i*. However, the situation with the tetrahedron is different in that carrying out the same symmetry operation – in this case passing each of the four ligands through the metal ion to an equivalent point on the other side – will result in a structure which, although still a tetrahedron, looks as if the original has been rotated to a new position. In this case the object *does not* possess the center of inversion, *i*. Quantum mechanically, the presence or absence of *i* in a metal complex has a significant effect on the intensity of the *d-d* transitions for the complex. Consider a *d-d* transition with $\Delta l = \Delta S = 0$ for two complexes, one of which is an octahedral complex and the other which has tetrahedral geometry. Experimentally, it is found that all of the transitions for the tetrahedral complex, which does not possess the symmetry element *i*, are more intense (they are more allowed) than are the transitions for the octahedral complex, which possesses *i*.

Clearly, the intensities of bands observed in transition metal complexes provide important information on the selection rules operating in the transition, which ultimately paves the way for assigning the bands to specific transitions in the energy-level diagram of the compound. A summary of the type of transition, its expected intensity and an example of the type of complex exhibiting the transition is given in Table 1.4. While the total integrated area under an absorption band is the quantity that is proportional to the probability that the transition will occur, all absorption bands regardless of their origin have approximately the same ratio of band width to band height. This means that $\varepsilon_{max}$, the molar extinction coefficient at the maximum of the band in units of $M^{-1}$ cm$^{-1}$, is a good measure of the intensity (probability) of the transition and thus is a useful metric for determining which selection rules apply to a transition.

**Table 1.4** Absorption properties of metal complexes.[a]

| Type of transition | $\Delta l$ | $\Delta S$ | Center of inversion, $i$ | $\varepsilon_{max}$ ($M^{-1}$ cm$^{-1}$) | Example complexes[b] |
|---|---|---|---|---|---|
| Laporte-forbidden Spin-forbidden | 0 | ≠0 | yes | <1 | $[Mn(H_2O)_6]^{2+}$ $O_h$, $S = 5/2$, $3d^5$ |
| Laporte-forbidden Spin-allowed | 0 | 0 | yes | 1–100 | $[Ru(H_2O)_6]^{2+}$ $O_h$, $S = 0$, $4d^6$ |
| Laporte-forbidden Spin-allowed | 0 | 0 | no | 100–1000 | $[NiCl_4]^{2-}$, $T_d$, $3d^8$ |
| Laporte-allowed Spin-allowed | ≠0 MLCT LMCT | 0 | no | 1000–50 000 | $[MnO_4]^-$, $T_d$, $3d^0$ $[AuCl(terpy)]^{2+}$, *s.p.*, $S = 0$, $5d^8$ |

[a]The ranges of molar absorbtivity, $\varepsilon$, given are considered *approximate.* Values outside these ranges have been observed for the various types of transition.
[b]Abbreviations: $O_h$, octahedral; $T_d$, tetrahedral; *s.p.*, square planar; *terpy*, 2,2′,2′′-terpyridine.

### 1.4.2 Absorption Spectra of Multi-Electron Systems

Analysis of the spectrum of a compound with a $d^1$ electronic configuration, after accounting for distortions due to the Jahn–Teller effect, proved to be relatively simple and straightforward. However, for complexes with more than one *d*-electron – indeed, for most of the known metal complexes – the analysis of spectra is more complicated. The problem with multi-electron systems is that once there is more than one electron in a given 'shell' or level of the atom (or ion), quantum mechanics dictates that not all spin and orbital angular momentum values for the system are possible. For example, suppose that the orbital motion of an electron about the nucleus of an atom is represented by a spinning bicycle tire with an axel or rod about which the tire is spinning. In a nonquantum mechanical world, the tire could spin with any angular velocity, setting up an angular momentum vector, $l_i$, with any magnitude, perpendicular to the angular velocity; that is, coincident with the axel of the spinning tire. Assume that for a multi-electron case there are many such tires, each with its axel randomly oriented in a different direction in space. The problem with this picture is that quantum mechanics simply does not allow all possible angular velocities or orientations of $l_i$, and specifies that all of the vectors must be of a certain magnitude and must couple in such a way that only certain resultant vectors, $L$ (where $L$ is the vector sum of all $l_i$) are allowed. This is called *Russell–Saunders* (R-S) coupling, and in simple terms it means that only certain angular velocities and orientations of the vectors are allowed. Not only are there restrictions on the orbital motion of the electron about the nucleus, but if the electron is considered a particle spinning on its axis, the spinning velocity generates a spin moment, $s_i$, which is perpendicular to the spinning motion. Quantum mechanics specifies that not all $s_i$ are allowed, and that they must couple to give a resultant $S$ which itself is quantized; that is, only certain values of $S$ are allowed. To complicate matters further, $L$ and $S$, which characterize the orbital and spin motion, respectively, can couple with each other to produce a resultant vector, $J$, which is characterized by the spin-orbit coupling constant, $\lambda$ (not to be confused with wavelength, which is denoted by the same Greek letter). If the metal atom is relatively light, like the elements of the first-row transition series, coupling between $L$ and $S$ is generally weak, and $|\lambda|$ is in the range 50 to 800 cm$^{-1}$, which is relatively small. This means that the system can be described by $L$ and $S$ because their coupling together to define $J$ is weak. However, for heavier elements like those in the third-row transition series and

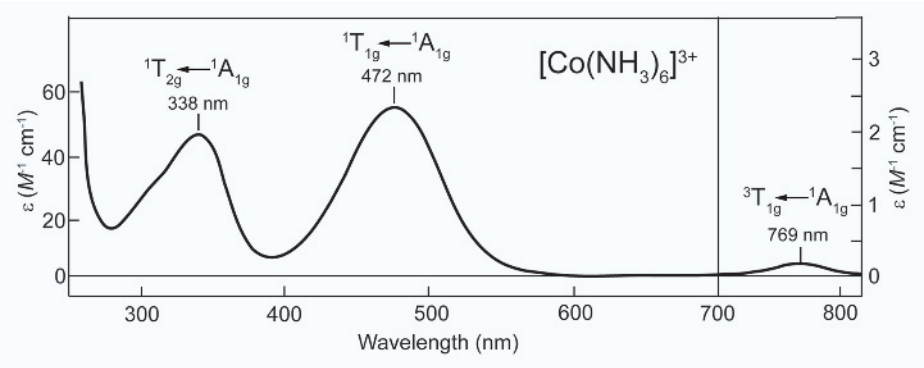


**Figure 1.17**

Absorption spectrum of $[Co(NH_3)_6]^{3+}$ in water. High-energy part adapted from Riordan, A.R., *et al.*, (2005) Spectrochemical Series of Cobalt(III). An Experiment for High School Through College. *Chem. Educator*, **10**, 115–119; low-energy part adapted from Lever, A.B.P., *Inorganic Electronic Spectroscopy*, 1968, Elsevier.

the lanthanides and actinides, $|\lambda|$ is greater than $10^3$ cm$^{-1}$. With large $|\lambda|$, $l$ and $s$, orbital and spin angular momenta associated with a single electron couple together to give $j$ for a single electron. The coupling of the $j$ vectors to produce the resultant $J$ gives rise to a new coupling scheme, called *jj coupling*, for which only $J$ has real physical meaning.

All of this quantum mechanical coupling ends up producing a series of states or levels in the energy level diagram that determines which absorptions will occur in the absorption spectrum. The individual states in the diagram carry designations like, $^1A_{1g}$, $^3T_{2g}$, and so forth, which characterize the number of unpaired electrons associated with the state (the superscript) and the 'symmetry' of the state (the upper-case letter and subscript) – information that is ultimately traceable back in a complicated way to combinations of the electronic configurations given for the various $d^1$–$d^9$ cases listed in Table 1.3. While deriving and explaining these spectral diagrams is well beyond the scope of presentation here, the crystal field splitting parameter, $\Delta_o$, which is the key parameter controlling the stability and reactivity of metal complexes, can be obtained from the absorption spectrum of the compound by using the energy level diagrams.

Figure 1.17 shows the absorption spectrum of $[Co(NH_3)_6]^{3+}$, which contains six ammonia ligands bonded in an octahedral array to $Co^{3+}$, $3d^6$ ($S = 0$). This complex exhibits three absorption bands at 769 nm (0.2), 472 nm (56) and 338 nm (46), which are the *lowest-energy d–d* absorptions for the complex [3]. In listing the bands, it is customary that the wavelength of the band maximum in nanometers ($10^{-9}$ m) be given, followed by the molar extinction coefficient, $\varepsilon$, in units of $M^{-1}$ cm$^{-1}$ in parentheses. Inspection of the absorption spectrum for $[Co(NH_3)_6]^{3+}$ reveals that the two highest energy bands, labeled $^1T_{2g} \leftarrow {}^1A_{1g}$ and $^1T_{1g} \leftarrow {}^1A_{1g}$, have intensities (values of $\varepsilon_{max}$) consistent with a Laporte-forbidden spin-allowed transitions (Table 1.4). These bands are due to a transition between two energy levels which have the same spin; that is, the net spin of the system does not change in the transition. The lowest energy band which is very weak, labeled $^3T_{1g} \leftarrow {}^1A_{1g}$, has an intensity consistent with a Laporte-forbidden, spin-forbidden transition (Table 1.4), indicating that the net spin changes in the transition. Crystal field theory shows that the critical band for determining $\Delta_o$ is the *lowest energy Laporte-forbidden spin-allowed transition*; that is, $^1T_{1g} \leftarrow {}^1A_{1g}$, at 472 nm (21 186 cm$^{-1}$) which, after carrying out crystal field calculations, gives $\Delta_o = 22\,870$ cm$^{-1}$, a value that is near in magnitude to the location of the

$^1T_{1g} \leftarrow {}^1A_{1g}$ transition. Since $E = h\nu = hc/\lambda = hc\Delta_o$, where $h$ is Planck's constant, $c$ is the speed of light and $\Delta_o$ is the crystal field splitting parameter, the energy splitting between the $t_{2g}$ and $e_g$ levels for a *single molecule* of $[Co(NH_3)_6]^{3+}$ is $4.55 \times 10^{-19}$ J which, when multiplied by Avogadro's number, gives ~274 kJ mol$^{-1}$ for a *mole* of $[Co(NH_3)_6]^{3+}$ molecules. By comparison, the dissociation energy for the average carbon–carbon bond in an organic compound is ~400 kJ mol$^{-1}$, showing that the CFSE for $[Co(NH_3)_6]^{3+}$ is substantial.

It emerges that the value of $\Delta_o$ can be roughly estimated for all high- and low-spin $d^1$–$d^4$ and $d^6$–$d^9$ cases using the location of the absorption band corresponding to the *lowest-energy spin-allowed Laporte-forbidden* transition for the complex. Since high-spin $d^5$ ($S = 5/2$) has no spin-allowed transitions, approximate calculations of $\Delta_o$ are less straightforward but can also be done using CF theory. Since the splitting for the tetrahedral arrangement of ligands is the inverse of the octahedral case, the location of the lowest-energy spin-allowed transition for tetrahedral complexes is also a good measure of the splitting between the $e$ and $t_2$ levels of the tetrahedral complex, which in this case is $\Delta_t$.

An important message from this analysis is that CF theory does a good job of explaining the optical properties of transition metal complexes. With absorption data for the complex and knowledge of basic selection rules, an approximate value of the crystal field splitting parameter $\Delta$ can be determined. Since $\Delta$ is a measure of the thermodynamic stability of the complex, it influences the rate at which the compound undergoes a substitution reaction (thermodynamic stability roughly correlates with activation energy), which in a pharmaceutical context is often the critical factor determining the potential of a compound as a useful drug or diagnostic agent.

## Box 1.3 Optical Activity, ORD/CD

Optically active compounds rotate the plane of *linearly polarized light* and interact with another form of light called *circularly polarized light*. These two properties are important not only for characterizing the optical properties of these compounds but also for studying how they interact with other chiral substances such as proteins and DNA.

While a detailed description of the properties of light is beyond the scope of presentation here, one way to think about light is that it consists of oscillating electric and magnetic fields that are perpendicular to each other and are traveling through space. In normal unpolarized light, these fields are oriented in every possible direction perpendicular to the direction of travel, but if the light is passed through a transparent device called a *polarizer*, only fields lying in one plane exit the polarizer, which produces *plane-polarized light*. If the magnitude of the electric field were represented by an arrow, the strength of the field would oscillate with time (distance) in one plane in a sine wave form, as shown in Figure 1.18. When plane-polarized light traverses a sample that is optically active, the light that exits the sample has its plane of polarization rotated by an amount related to the number of optically active molecules or chiral entities in the sample. The amount of rotation, measured in degrees, is the *observed rotation*, $\alpha$. If the light beam is moving toward the observer and if the plane of rotation of light is to the *right* as it exits the sample, $\alpha$ is positive and the sample is said to be *dextrorotatory* (*d*). For the opposite case, $\alpha$ is negative and the sample is said to be

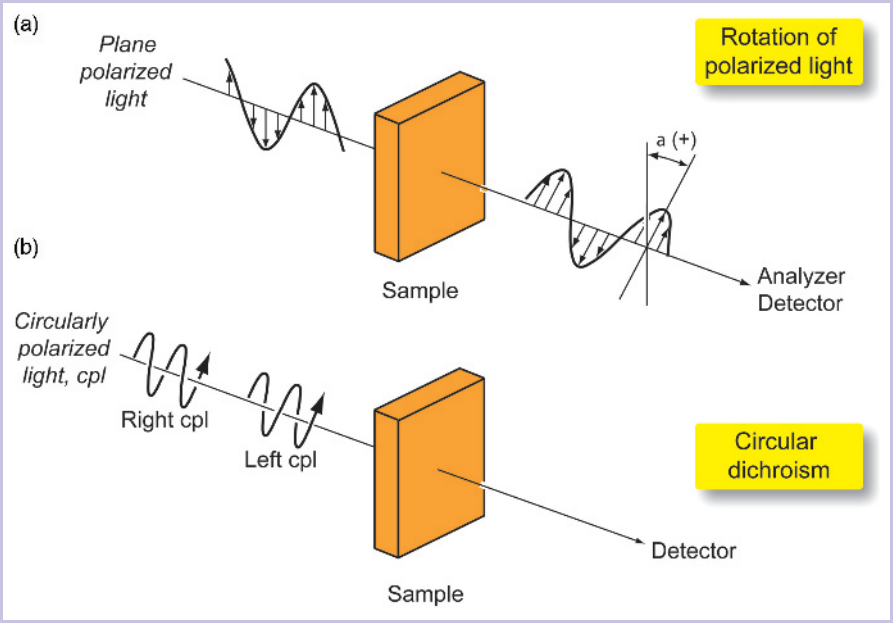


**Figure 1.18**

(a) Measurement of the rotation of linearly polarized light. The electric vector of light, indicated by an arrow, changes in magnitude with time (distance) in the manner shown. The angle of rotation of the plane of polarization, $\alpha$, is positive if the plane of light after passing through the optically active sample is rotated to the left as viewed by an observer facing the light; that is, if the light is moving toward the observer. The angle of rotation is measured by an analyzer/detector. (b) Schematic of the circular dichroism measurement. Left and right circularly polarized light (cpl), indicated as left cpl and right cpl, pass through an optically active sample, with one form being absorbed by the sample to a greater extent than the other form. The absorbance of each form is measured by a detector which is 'locked into' the form of light being generated.

*levorotatory* (*l*). The value of $\alpha$ can easily be measured by rotating a second polarizer in front of the detector and noting the angle of the polarizer at which light reaching the detector is at its maximum value.

The two quantities that are usually used to denote the optical rotation of an optically active compound in solution are the *specific rotation*, *[α]* [Eq. (1.3)] and the *molar rotation*, *[ϕ]* [Eq. (1.4)].

$$\text{Specific rotation} = [\alpha] = \frac{\alpha}{dc} \tag{1.3}$$

$$\text{Molar rotation} = [\phi] = \frac{100\alpha}{lM} \tag{1.4}$$

In the expression for specific rotation, $\alpha$ is the observed angle of rotation in degrees, $d$ is the path length in decimeters of the sample ($d = 10$ cm), and $c$ is the concentration of the optically active substance in solution (in g cm$^{-3}$). For molar rotation, $\alpha$ is as above, $l$ is the path length in cm, and $M$ is the concentration of the solute in mol l$^{-1}$.

An interesting property of optically active compounds is that both the sign and the magnitude of rotation of plane-polarized light depend on the relative location of an electronic absorption band for the compound and the wavelength, $\lambda$, of light being

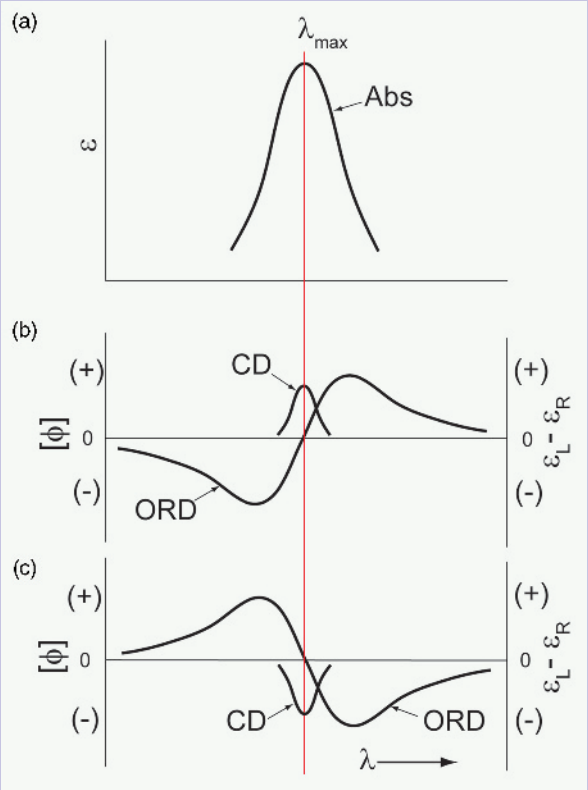


**Figure 1.19**
(a) Absorption curve, (b) optical rotatory dispersion (ORD) and circular dichroism (CD) curves for an enantiomer exhibiting a positive Cotton effect. (c) ORD and CD curves for the mirror-image enantiomer exhibiting a negative Cotton effect.

used to make the rotation measurement. This effect, which is called *optical rotatory dispersion*, *ORD*, is shown for two enantiomers in Figure 1.19. As is evident from the figure, the value of $[\phi]$ associated with one of the enantiomers (Figure 1.19b) is positive on the long-wavelength side of $\lambda_{max}$ (the maximum of the absorption band), and negative on the short-wavelength side, giving rise to a *positive* ORD curve. For the other enantiomer (Figure 1.19c), the opposite is true, in that $[\phi]$ is negative on the long-wavelength side and positive on the short-wavelength side, producing a *negative* ORD curve. Both ORD curves pass through a common point at $\lambda_{max}$ when $[\phi]$ is zero.

The second type of measurement commonly employed for studying optically active compounds is *circular dichroism* or *CD*. In this technique, the electric vector of light is made to move in a coil or helix and two forms are possible: *left circularly polarized light* and *right circularly polarized light* (Figure 1.18). While the details of how this light form is generated will not be given, it starts with plane-polarized light, which is passed through a device called a 'quarter wave plate.' This changes the phasing between components of plane-polarized light by 90° (one quarter of 360°), and the result is that the electric vector moves in a helical fashion with time (distance traveled).

By advancing or retarding one of the components relative to the other by 90°, the light emanating from the quarter wave plate is right circulary polarized at one instant in time and left circularly polarized at the next instant, which in effect alternately sends right- and left-hand coils of light at the sample in a continuous stream. Since a given enantiomer will interact with each of these light forms differently, and the detector can be electronically 'locked in' with the form of light being generated, the detector is able to directly measure the *absorbance* by the sample of each light form. The difference, $\Delta A = A_{\mathrm{L}} - A_{\mathrm{R}}$, is related through the Beer–Lambert law to the *molar circular dichroism*, $\Delta\varepsilon$, using Eq. (1.5), where $A_{\mathrm{L}}$ and $A_{\mathrm{R}}$ are the absorbances and $\varepsilon_L$ and $\varepsilon_R$ are the molar absorptivities of left and right cpl by the sample, respectively; the quantity $l$ is the path length in cm, and $M$ is the concentration in mol $\mathrm{l}^{-1}$.

$$\text{Molar circular dichrosim} = \Delta\varepsilon = \varepsilon_L - \varepsilon_R = \frac{A_L - A_R}{lM} \tag{1.5}$$

For historical reasons, another way to report CD is to express the effect using the *molar ellipticity*, $[\theta]$ [Eq. (1.6)], where $\psi$ is the observed ellipticity, with both measures of CD – $[\theta]$ and $\Delta\varepsilon$ – being related to each other through Eq. (1.7).

$$\text{Molar ellipticity} = [\theta] = \frac{100\psi}{lM} \tag{1.6}$$

$$[\theta] = 3298(\varepsilon_L - \varepsilon_R) \tag{1.7}$$

The relationship between absorption, ORD and CD curves for two enantiomers is shown in Figure 1.19. As is evident from the figure, the CD curve is similar in shape to the absorption curve, but unlike the latter the CD band can be either negative or positive in sign, and the width of the band is narrower than the width of the absorption band. It is also important to note that a positive CD curve is coupled to a positive ORD curve, and together the two curves constitute a *positive Cotton effect* (Figure 1.19b), named after the French physicist who discovered the phenomenon. The opposite set of CD and ORD curves (Figure 1.19c) constitute a *negative Cotton effect*.

The set of curves shown in Figure 1.19 is for a single isolated absorption band of an optically active compound, but in reality absorption bands of compounds caused by electronic transitions are most often overlapped. Since each absorption band can exhibit a positive *or* a negative Cotton effect, the CD spectrum of a pure enantiomer can be complicated and exhibit a number of CD bands, each of which can be either negative or positive and have different areas (band intensities). If both enantiomers of a compound are optically pure, or if they are not pure but the level of optical purity is the same for both, the CD spectrum of both, except for sign, will be identical; that is, the curves will appear as mirror images of each other. If the solution contains equal molar amounts of both enantiomers, the optical activity effects of both will exactly cancel and there is no net optical activity and no Cotton effect; that is, the sample will be optically inactive.

Since the ORD curve covers a much larger wavelength range than the CD curve, and positive and negative ORD effects from many absorption bands will be strongly overlapped, ORD is not often used in the study of optically active compounds. However, measurement of the specific or molar rotation at a single wavelength, which is an intrinsic property of a pure material, is often carried out. Usually, the wavelength

for the measurement is 589 nm, often denoted by the letter 'D', which stands for two closely-lying 'D-lines' in the emission spectrum of gaseous sodium. This wavelength of light is the strong yellow radiation emitted by a sodium vapor lamp. If a compound only has an absorption band in the UV region of the spectrum and no bands in the visible region, the ORD curve for the band in the UV region will 'tail' into the visible region, making the measurement of rotation at 589 nm possible. The instrument used to measure optical rotation is called a *polarimeter*. It is conventional to give the temperature and wavelength employed on the parameter being reported, for example $[\alpha]_{\mathrm{D}}^{25} = -31.2°$.

While it is true that enantiomers have CD and ORD curves that are exact mirror images of each other, it is generally not easy to determine which Cotton effect corresponds to which absolute configuration of the compound. This is because the interaction of chiral light with chiral molecules – especially in the case of coordination compounds – is still poorly understood, and predicting the spatial arrangements of atoms in a molecule on the basis of optical activity effects alone is not easy to do.

## 1.5 Magnetic Properties of Metal Complexes

As we have seen, the quantity $S$ is a useful way to indicate the number of unpaired electrons on the metal ion in a complex. If a metal complex has no unpaired electrons on the metal ion, $S = 0$, and if it is placed near a magnetic field, the applied field will induce circulation of electronic currents, which cause the substance to be repelled by the field. In this case, the substance exhibits *diamagnetism* and is said to be *diamagnetic*. However, if the metal ion in the complex has one or more unpaired electron, $S \neq 0$, placing the compound near a magnetic field will set up an electronic current, causing it to be *drawn into* the field. This property of being drawn into the field is termed *paramagnetism* and the compound is referred to as being *paramagnetic*. In terms of the strengths of the two forces, the paramagnetic force, on a per-atom basis, is the stronger of the two.

The degree to which the material exhibits either effect is called the *effective magnetic susceptibility* of the material, which is denoted by the quantity $\mu_{\mathrm{eff}}$ and which is given in a unit called the *Bohr magneton* (BM), where $1\ \mathrm{BM} = 9.27 \times 10^{-24}\ \mathrm{JT}^{-1}$. While $\mu_{\mathrm{eff}}$ can vary in a complicated way with temperature, paramagnetic complexes of the first-row transition metal elements have values of $\mu_{\mathrm{eff}}$ that are relatively independent of T near room temperature. However, for complexes of the second- and third-row transition metal elements, $\lambda$, which is the spin-orbit coupling constant, is large and for these complexes $\mu_{\mathrm{eff}}$ is usually quite sensitive to temperature over all temperature ranges.

The general approach for determining the number of unpaired electrons of a paramagnetic complex is to measure the force with which a sample of the material is pulled into a magnetic field. After making corrections for diamagnetic effects associated with the ligands, the effective magnetic susceptibility, $\mu_{\mathrm{eff}}$, associated with the paramagnetic metal ion can be obtained. This value can be compared with the magnetic susceptibility, calculated using a simple formula which assumes that all of the paramagnetism is due only to the spin moments of the unpaired electrons on the metal ion, with no orbital motion. This *spin-only magnetic susceptibility*, $\mu_{\mathrm{so}}$, is given in two forms: Eq. (1.8), which is in terms of $S$, and Eq. (1.9), which is in terms of the number of unpaired electron on the metal ion, $n$.

For example, for a complex with three unpaired electrons, $n = 3$ and $S = 3/2$, which gives $\mu_{so} = 3.87$ BM.

$$\mu_{so} = 2\sqrt{S(S+1)}\text{BM} \tag{1.8}$$

$$\mu_{so} = \sqrt{n(n+2)}\text{BM} \tag{1.9}$$

Experimentally, it is found that metal ions in complexes having an electronic configuration that has only one way to arrange the electron spins without changing the net spin of the system, for example $Co^{2+}$ in a tetrahedral field with the electronic configuration $e^4t^3$, have values of $\mu_{eff}$ that are nearly the same as $\mu_{so}$. This means that the only property contributing to the observed paramagnetism of the compound are the spins associated with the unpaired electrons on the metal ion. However, for metal complexes with more than one way to arrange electrons spins without changing the net spin of the system – for example, $Fe^{2+}$ in a tetrahedral field with the electronic configuration $e^3t^3$ or $Fe^{3+}$ in a octahedral field with the electronic configuration $t_{2g}^5e_g^0$ – the value of $\mu_{eff}$ is usually *larger* than $\mu_{so}$. This is because there are really two important contributions to the paramagnetism for the sample: one contribution is associated with the spin moment of the electron, but the second is associated with the orbital motion of the electron about the nucleus. For example, for $T_d$, $Fe^{2+}$, the $e^3t^3$ configuration can be written in *two* ways: $d^2_{x^2-y^2}$, $d^1_{z^2}$, $d^1_{xz}$, $d^1_{yz}$, $d^1_{xy}$ (a) or $d^1_{x^2-y^2}$, $d^2_{z^2}$, $d^1_{xz}$, $d^1_{yz}$, $d^1_{xy}$ (b), both of which have identical energies. Inspection of these two electronic configurations reveals that the unpaired electron in the $e$ level of (a) has moved from the $d_{z^2}$ orbital to the $d_{x^2-y^2}$ orbital of (b). While this may seem trivial, it in effect constitutes a motion of the unpaired electron from one orbital to the other; that is, the electron appears to *rotate* about the nucleus. This rotation produces a magnetic moment that adds to magnetic moments produced by the spins, which increases the magnetic susceptibly above the value calculated from the spin-only formula. This orbital contribution is especially important for configurations in which there three ways to arrange electrons without changing the net spin or total energy of the system. An example of this case is low-spin $d^4$ in an $O_h$ crystal field, $t_{2g}{}^4e_g{}^0$, which can have the two paired electrons in either $d_{xz}$, $d_{yz}$ or $d_{xy}$ which produces a larger orbital contribution to $\mu_{eff}$. Fortunately, the contribution made by the orbital motion is not so large so as to preclude using the simple spin-only formula to determine the value of $S$, which gives the number of unpaired electrons for the complex from $\mu_{eff}$.

The above description of magnetic properties of complexes assumes that the ions with unpaired electron spin are well separated from each other, and that there is no interaction between the spins; that is, the systems are said to be *magnetically dilute*. However, for certain substances, such as iron oxides, which are widely used in nanomedicine applications (see Chapter 10), the iron ions are embedded in an oxide crystal lattice in which the ions are close to one another. This proximity allows the individual magnetic moments of the ions to couple with one another to produce a large net magnetic moment. While the degree of coupling varies in a complicated way with the nature of the paramagnetic ions involved, their separation in the lattice and the physical size of the particle, one case – called *ferromagnetism* – has a large group of spin moments oriented in the same direction, resulting in a large net magnetic moment, which produces a permanent magnetic field for the material. These substances are referred to as *ferromagnetic* materials. Particles in the nanometer size range having this property are referred to as being *superparamagnetic nanoparticles*.

## 1.6 Structure and Reactivity of Metal Complexes

### 1.6.1 Forward and Reverse Rates and Equilibrium

Most of the metal complexes that have found their way into medicine exert their biological effects by reaction with nucleophiles present in the body. While metal complexes can react through a variety of different mechanisms, a substitution reaction, in which a ligand is displaced by an attacking ligand, is the most common. In the hypothetical reaction shown in Eq. (1.10), one of the ligands originally attached to the metal ion is replaced by the attacking nucleophile to form a product.

$$ML_xX + Y \underset{k_{-2}}{\overset{k_2}{\rightleftharpoons}} ML_xY + X \tag{1.10}$$

Suppose that an attacking nucleophile, Y, is added to a solution containing $ML_xX$. At $t = 0$, the time of addition, there can be no product $ML_xY$ and the concentration of $ML_xX$ is its initial concentration, $[ML_xX]_0$, with the initial concentration of Y being $[Y]_0$. [*Note*: While activities are required for rate and equilibrium expressions, this work will assume that activities of substances are equal to their concentrations, as would be the case when concentrations approach zero, and 'concentration' will be used throughout the text.] As time passes, the original concentration of starting material, $ML_xX$, decreases at some rate and the concentration of the product, $ML_xY$, increases at the same rate. This is depicted in Figure 1.20, which shows how the ratios $[ML_xX]/[ML_xX]_0$ and $[ML_xY]/[ML_xX]_0$ for the reaction change with time. The rate of decrease of $ML_xX$ as a function of time is given by the *rate law* [Eq. (1.11)]:

$$\text{rate} = k_2[ML_xX][Y] \tag{1.11}$$

In this expression, $k_2$ is the second-order *forward rate constant*, and $[ML_xX]$ and $[Y]$ are the concentrations of $ML_xX$ and Y, respectively. If there is some mechanism by which starting material can be reformed from the product, the reaction will eventually reach a point where the concentrations of all of the components in the reaction medium will not change with

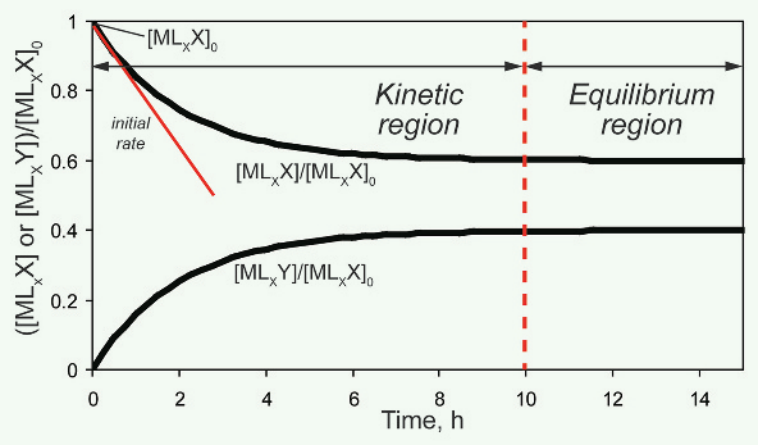


**Figure 1.20**

Rate curves, concentration versus time, for the reaction of $ML_xX$, starting concentration $[ML_xX]_0$, with nucleophile Y to form product $ML_xY$.

time and the system is said to be at *equilibrium*. In the hypothetical reaction shown in Figure 1.20, equilibrium is reached after ~10 hours. In a similar way to the process in the forward direction, the rate in the reverse direction is given by the *rate law* [Eq. (1.12)]:

$$\text{rate} = k_{-2}[\text{ML}_\text{x}\text{Y}][\text{X}] \tag{1.12}$$

In this expression $k_{-2}$ is the second-order *reverse rate constant* and $[\text{ML}_\text{x}\text{Y}]$ and [X] are the concentrations of $\text{ML}_\text{x}\text{Y}$ and X, respectively.

At small intervals of time – that is, just after the nucleophile Y has been added to the medium – the observed rate of disappearance of $\text{ML}_\text{x}\text{X}$ is said to be the *initial rate* of disappearance, which is the *initial slope* of the rate curve for $\text{ML}_\text{x}\text{X}$. In this region of the rate curve there is very little product, and the possibility of making some starting material through the reaction of X with $\text{ML}_\text{x}\text{Y}$ [Eq. (1.10)] is negligible. Since the early part of the rate curve contains no significant 'back reaction', this part of the curve can be used to calculate the true forward *rate constant*, $k_2$, for the reaction from the *initial rate* of disappearance of $\text{ML}_\text{x}\text{X}$, and the initial concentrations, $[\text{ML}_\text{x}\text{X}]_0$ and $[\text{Y}]_0$, according to Eq. (1.13):

$$\text{Initial rate} = k_2[\text{ML}_\text{x}\text{X}]_0[\text{Y}]_0 \tag{1.13}$$

When the system reaches equilibrium, the rates in the forward and reverse directions must be the same to give Eq. (1.14), in which the concentrations are the values at equilibrium, indicated by $[\text{ML}_\text{x}\text{X}]_\text{eq}$, $[\text{ML}_\text{x}\text{Y}]_\text{eq}$, $[\text{X}]_\text{eq}$ and $[\text{Y}]_\text{eq}$. Rearranging this expression gives Eq. (1.15), which shows the relationship between the equilibrium concentrations, the equilibrium constant, $K$, and the forward and reverse rate constant for the reaction. Since the free energy, $\Delta G$, is related to the equilibrium constant through Eq. (1.16) or its exponential form [Eq. (1.17), the free energy of the reaction can be calculated from $K$ and the temperature. Experimentally, a common way to obtain $k_{-2}$ is to determine $k_2$ by measuring the initial rate of the reaction, allowing the reaction to reach equilibrium, and determining $K$ through the equilibrium concentrations:

$$k_2[\text{ML}_\text{x}\text{X}]_\text{eq}[\text{Y}]_\text{eq} = k_{-2}[\text{ML}_\text{x}\text{Y}]_\text{eq}[\text{X}]_\text{eq} \tag{1.14}$$

$$\frac{k_2}{k_{-2}} = \frac{[\text{ML}_\text{x}\text{Y}]_\text{eq}[\text{X}]_\text{eq}}{[\text{ML}_\text{x}\text{X}]_\text{eq}[\text{Y}]_\text{eq}} = K \tag{1.15}$$

$$\Delta G = -RT \ln K \tag{1.16}$$

$$K = e^{-\frac{\Delta G}{RT}} \tag{1.17}$$

All of the above follows well-developed theory for a simple chemical system on its way to, and eventually reaching, equilibrium. The conditions in a cell or the body are obviously much different, in that equilibrium in the chemical sense is never achieved unless death occurs. Nonetheless, the principles covered still apply to the early time course of events that must take place when a metallo-drug interacts with a cellular target such as a protein or DNA.

### 1.6.2 Water Exchange Rates for Metal Ions

An important indicator or 'benchmark' of the rate at which a metal complex will be expected to undergo a substitution reaction is the rate at which the metal ion in the complex exchanges a bound water molecule with another water molecule that is free in bulk water. This rate, called the *water exchange rate*, is easily determined by measuring how fast a metal-bound

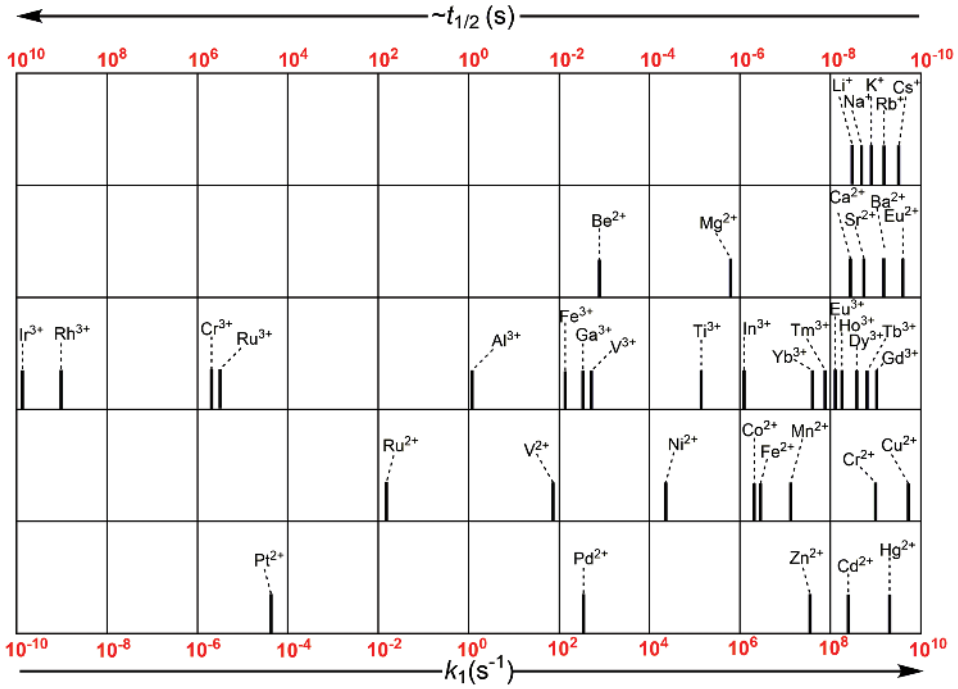


**Figure 1.21**

Water exchange rate constants and half-lives for some metal ions at 25 °C. Adapted from Helm, L. and Merbach, A.E. (1999) Water Exchange on Metal Ions: Experiments and Simulations. *Coord. Chem. Rev*., **187**, 151–181. Copyright 1999, with permission from Elsevier. Reproduced with permission of Elsevier.

water molecule having naturally occurring $^{16}O$ water can be replaced with a water molecule having isotopically labeled $^{17}O$ water [Eq. (1.18)]:

$$[M(H_2{}^{16}O)_n]^{z+} + H_2{}^{17}O \underset{k_{-2}}{\overset{k_2}{\rightleftharpoons}} [M(H_2{}^{16}O_{n-1})(H_2{}^{17}O)]^{z+} + H_2{}^{16}O \tag{1.18}$$

Water exchange kinetics are measured by dissolving a metal aqua complex having bound $^{16}O$ water in water that has some water molecules labeled with $^{17}O$ and using NMR ($^{17}O$ has a nuclear spin of $^1/_2$) to observe the rate at which unbound $^{17}O$ becomes bound to the metal ion. Figure 1.21 shows the water exchange rates for a number of metal ions, measured by $^{17}O$ NMR and other techniques [4]. The pseudo first-order exchange rate constants, $k_1$, given along the bottom of the figure, are related to the half-lives $t_{1/2}$ values along the top of the figure using Eq. (1.19):

$$t_{1/2} = \frac{0.6931}{k_1} \tag{1.19}$$

The striking feature about Figure 1.21 is that the rate constant, $k_1$, varies by 19 orders of magnitude, ranging from $10^{-10}$ $s^{-1}$ for $Ir^{3+}$ to $10^{9}$ $s^{-1}$ for $Cs^+$. While the latter ion exchanges one of its bound water molecules with bulk water a *billion* times per second, the former exchanges its water molecules once every 300 years! Not surprisingly, a single bonding model cannot be used to explain all of the water exchange rates in Figure 1.21, but as will be evident in the following section, CF theory can be used to explain why some

rates are very slow, and simple electrostatic arguments can be used to explain why others in Figure 1.21 are very fast.

### 1.6.3 Transition State Theory, the Kinetic Rate Constant and Equilibrium

Observations made by Arrhenius and others showed that the rate constant for any reaction, $k$, is given by Eq. (1.20) and its exponential form [Eq. (1.21)]:

$$\ln k = -\left(\frac{E_a}{RT}\right) + \ln A \tag{1.20}$$

$$k = Ae^{-\frac{E_a}{RT}} \tag{1.21}$$

In this empirical expression, called the *Arrhenius equation*, $E_a$ is the *activation energy*, $A$ is the pre-exponential factor, $R$ is the gas constant, and $T$ is the absolute temperature. The Arrhenius equation shows that while an increase in temperature *increases* the rate constant for the reaction, and thus the rate of the reaction, an increase in $E_a$ *decreases* the rate constant for the reaction.

In an attempt to more clearly define the factors that influence the rate of a reaction, Eyring and others analyzed the progress of chemical reactions using *transition state theory*. With this theory, a reaction is discussed using a plot with the *reaction coordinate* as the x-axis and the free energy as the y-axis. In order for a reactant to be converted into a product, the reaction must pass through a maximum in the energy, which is denoted as the *transition state* or the *activated complex* (Figure 1.22). Transition state theory considers the energy barrier between the reactants and the products as the *free energy of activation*, which if the reaction is moving in the 'forward' direction is given the designation $\Delta G^{\ddagger}_{f}$. Since in Figure 1.22 the reactants are less stable than the products, the free-energy change for the reaction, $\Delta G_{rxn}$, is *negative*, which indicates that the reaction is thermodynamically favored in moving from left to right; that is, from reactants to products. If there is a route for products to return to reactants, the free energy of activation in the reverse, 'back', direction is $\Delta G^{\ddagger}_{b}$. Using Eq. (1.17), the equilibrium constant, $K$, for such a situation is greater than 1, and if

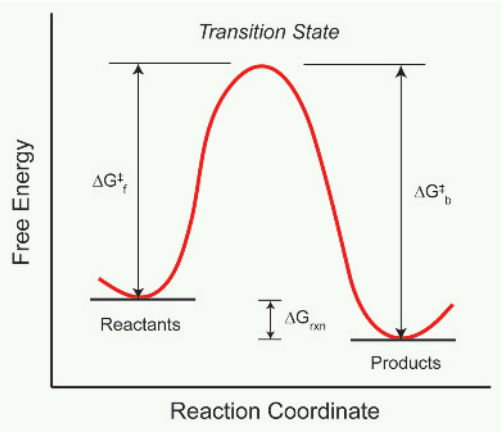


**Figure 1.22**
Reaction coordinate based on transition state theory for a reaction with $-\Delta G_{rxn}$.

enough time is allowed for the system to reach equilibrium, the concentration of products will be greater than the concentration of reactants.

The relationship between the kinetic rate constant, $k$, for a reaction and $\Delta G^{\ddagger}$ from transition state theory [Eq. (1.22)] is almost the same as with the Arrhenius equation, but the pre-exponential factor, $A$, in Eq. (1.21) is replaced with the product of a constant, $b$, and the temperature, $T$, in Eq. (1.22).

$$k = bTe^{-\frac{\Delta G^{\ddagger}}{RT}} \tag{1.22}$$

Like the Arrhenius equation, Eq. (1.22) shows that an increase in temperature *increases* the rate constant of the reaction, while an increase in the activation free energy, $\Delta G^{\ddagger}$, *decreases* the rate constant of the reaction. It is also clear that the rate constant $k$ in Eq. (1.21) has a slightly different temperature dependence than $k$ in Eq. (1.22), but the main temperature dependence for both is in the exponential terms.

The water exchange reaction for a metal ion can take place through one of two possible mechanisms. One mechanism, called the *associative mechanism* [Eq. (1.23)], involves a water molecule from bulk solvent adding to the metal ion to form a transient high-energy *seven-coordinate* transition state (activated complex), which ultimately decays to the product by losing a water molecule. A second mechanism, called the *dissociative mechanism* [Eq. (1.24)], involves a *five-coordinate* complex in the transition state, which ultimately captures a water molecule to give the product.

$$[M(H_2O)_6]^{z+} + H_2O \rightarrow [M(H_2O)_7]^{z+} \rightarrow [M(H_2O)_6]^{+z} + H_2O \tag{1.23}$$

$$[M(H_2O)_6]^{z+} \rightarrow [M(H_2O)_5]^{z+} + H_2O \rightarrow [M(H_2O)_6]^{z+} \tag{1.24}$$

For transition metal ions with large crystal field stabilization energy (CFSE), changing the structure of the complex from a six- to either a seven- (associative mechanism) or a five-coordinate (dissociative mechanism) structure is generally energy-expensive; that is, it costs energy to do this. Suppose for example the starting six-coordinate complex is $d^6$ ($S = 0$), which has CFSE = –2.4 $\Delta_o$ + 2$P$ (see Table 1.3), and the geometry of the activated complex is a seven-coordinate structure; that is, the associative mechanism. While the exact geometry of the transitions state is not known, a pentagonal bipyramidal structure is a reasonable supposition (Figure 1.1). From the one-electron energy levels of the $d$-orbitals in Table 1.1, a pentagonal bipyramidal structure with $S = 0$ would have CFSE of –1.548 $\Delta_o$ + 2$P$ relative to the spherical field. Taking the difference between these two quantities using the thermodynamic convention of *energy of the final state minus the energy of the initial state* [Eq. (1.23)], one obtains +0.852 $\Delta_o$, which shows that from the standpoint of CFSE, the change in geometry in moving from the six-coordinate octahedral structure to the seven-coordinate pentagonal bipyramidal transition state is *energetically unfavorable*; that is, discounting entropy, $\Delta G^{\ddagger}_{f}$ in Figure 1.22 is positive.

$$\Delta\text{CFSE} = (-1.548\ \Delta_o + 2P) - (-2.4\ \Delta_o + 2P) = +0.852\ \Delta_o \tag{1.25}$$

Performing a similar calculation for the structural change from a six-coordinate octahedral to a five-coordinate square pyramidal, a reasonable structure for the transition state gives a ΔCFSE of +0.4 $\Delta_o$, indicating that from the standpoint of crystal field effects, this *dissociative* process is also energetically unfavorable. Although factors other than simple crystal field effects are important in the rate of substitution of an ion, a useful guide is that

when CFSE for the metal complex is large – for example, $Ir^{3+}$ ($5d^6$, $S = 0$), $Rh^{3+}$ ($4d^6$, $S = 0$), $Cr^{3+}$ ($3d^3$, $S = 3/2$), $Ru^{3+}$ ($4d^5$, $S = 1/2$), $\Delta G^{\ddagger}_{f}$ is generally large and the rate constant for water exchange, through Eq. (1.21) or Eq. (1.22), is small. Similar arguments also apply to complexes with a four-coordinate square planar geometry, for example $Pt^{2+}$ ($5d^8$, $S = 0$). Square-planar $Pt^{2+}$ complexes are believed to substitute via an *associative* process [Eq. (1.24)] involving a five-coordinate transition state which, if the structure of the intermediate is square pyramidal, has a value of ΔCFSE for reaching the transition state that is positive. As is shown in Figure 1.21, these ions have relatively small water exchange rate constants, which is consistent with their large positive values of ΔCFSE. When $\Delta_o$ is small – which happens when the oxidation state of the metal ion is low and if the ion is in the first-row transition metal series – values of CFSE are small. In this case, CFSE of the starting complex and the ΔCFSE required to reach a transition state become less of a predictor of reaction rate, and other factors such as the organization of solvent in the solvation sphere of the complex become important in determining the reaction rates of the compound.

For main group cations that have filled outer electronic shells, there is no CFSE. For these ions, simple electrostatic considerations involving the *electrostatic potential* on the surface of the cation that contacts the water molecule can explain exchange rates. For example, if a cation has a large radius and a low net positive charge, the electrostatic potential on the surface of the cation (considered a sphere) that comes into contact with the dipole of the water molecule will be small, leading to a weak electrostatic bond between water and the cation. If the bond is weak, it will be easily broken, which will ultimately translate into rapid exchange of bound water molecules with those in solvent. Consider the series $Al^{3+}$, $Ga^{3+}$, $In^{3+}$, the series $Be^{2+}$, $Mg^{2+}$, $Ca^{2+}$, $Sr^{2+}$, $Ba^{2+}$ and the series $Li^{+}$, $Na^{+}$, $K^{+}$, $Rb^{+}$, $Cs^{+}$, which are given in order of *increasing* ionic diameter or, since the charge on the cation in each series is the same, in order of *decreasing* electrostatic potential on the surface of the cation. Since the smallest member of each series forms the strongest metal ion–water bond, it has the *largest* value of $\Delta G^{\ddagger}_{f}$ (Figure 1.21) and the smallest water exchange rate constant, $k$, through Eqs (1.21) and (1.22). The water exchange rate data given in Figure 1.21 show that $k$ increases with atomic number for each series, which indicates that the simple electrostatic argument given above is probably correct.

### 1.6.4 *Trans* Effect and Substitution Reactions

In even a brief presentation of the substitution properties of metal complexes, it is important to describe the *trans effect* observed for reactions of square planar compounds, especially those of $Pt^{2+}$, which are potent anticancer drugs. In simple terms, the *trans effect pertains to the ability of a ligand in a complex to direct substitution opposite, or trans, to itself.* This effect was discovered by Chernyaev [5], who after synthesizing many square planar complexes of $Pt^{2+}$ found that the presence of certain ligands attached to the metal ion had the ability to cause the loss of the group that was in the position *trans* to the ligand in a substitution reaction. As might be expected, not all ligands have the same strength in '*trans* directing ability' and ultimately a series, called the *trans effect series* (Table 1.5), was created to rank common ligands by their ability to direct an incoming group (nucleophile) to the coordination site *trans* to themselves. In this series, the ligand with the greatest *trans* directing ability is $CN^{-}$, while the one with the *weakest* ability is water, $H_2O$.

A number of models have been proposed to explain the *trans* effect and why a given ligand is where it is in the series, but ultimately none seems to provide an explanation of

**Table 1.5** The *trans* effect series.[a]

| $CN^- \sim CO \sim C_2H_4 > PH_3 \sim SH_2 > NO_2^- > I^- > Br^- > Cl^- > NH_3 \sim py > OH^- > H_2O$ |
|---|

[a]In this series, $CN^-$ is the strongest *trans* directing ligand and water is the weakest. This table is the series stated in text on p. 439 of Miessler, G.L., Tarr, D.A. (2004) *Inorganic Chemistry*, 3rd edn, Pearson Prentice Hall, Upper Saddle River, NJ.

the ranking of all of the ligands in the series. Early models focused on the structure of the reactants, and whether and to what extent groups that were *trans* to strong *trans* -directing ligands have their bonds lengthened. These models, which used thermodynamic arguments, assumed that if a bond was slightly longer in the starting complex it would be the bond broken in the substitution reaction. Other models, which were based on transition state theory, and thus provided a kinetic focus, addressed the structure of the transition state or activated complex in the reaction. These models considered how the *electronegativity* of groups and/or their ability to form π-bonds with the metal ion in the transition state affected which groups would be lost when the product was formed. While these models addressed the *trans* effect from the kinetic perspective – that is, they considered the nature of the transition state and discussed what happened in terms of the reaction coordinate – difficulties in estimating the electronegativities of groups and a lack of knowledge of the structure of the transition state made them somewhat difficult to use.

In order to illustrate how the *trans* effect series works, consider the syntheses of the important anticancer drug *cisplatin*, *cis*-diamminedichloroplatinum(II), and its less active isomer, *transplatin*, *trans*-diamminedichloroplatinum(II) (Figure 1.23) [6]. Note that when ammonia is incorporated into a metal complex as a ligand, scientific nomenclature requires that the term used in the name of the compound is 'ammine.' In the synthesis of cisplatin, which most often employs the *Dhara synthesis* [7] (Figure 1.24), a commercially available source of $Pt^{2+}$, potassium tetrachloroplatinate, $K_2[PtCl_4]$, is reacted with excess potassium iodide, KI, in water. Most of the evidence for reactions of this type shows that the mechanism is *associative*; that is, an iodide ion attacks the platinum ion as one of the bound chloride ligands leaves. This substitution occurs sequentially until all four chloride ligands have been replaced by iodide to form $[PtI_4]^{2-}$. In this reaction, the attacking ligand approaches the platinum ion via the unobstructed z-axis of $[PtCl_4]^2$; that is, it attacks the exposed $d_{z^2}$ orbital of the complex (see Figure 1.3) to produce a five-coordinate, most likely trigonal bipyramidal, transition state (see Figure 1.1). After $[PtCl_4]^{2-}$ has been converted to $[PtI_4]^{2-}$, the next step in the Dhara synthesis of cisplatin is to add two equivalents of ammonia, $NH_3$, to the tetra-iodo complex. Note that when addressing a group bound to a metal ion which is an anion, the suffix 'o' is added to the name of the group. The interesting feature of the product of this reaction is that that while two geometric isomers are possible, *cis* and *trans* (Figure 1.23), and the *former* is less *thermodynamically stable* than the *latter*,

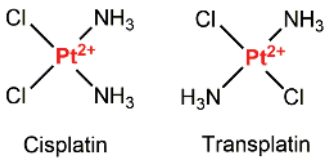


**Figure 1.23**
Structures of cisplatin and transplatin.

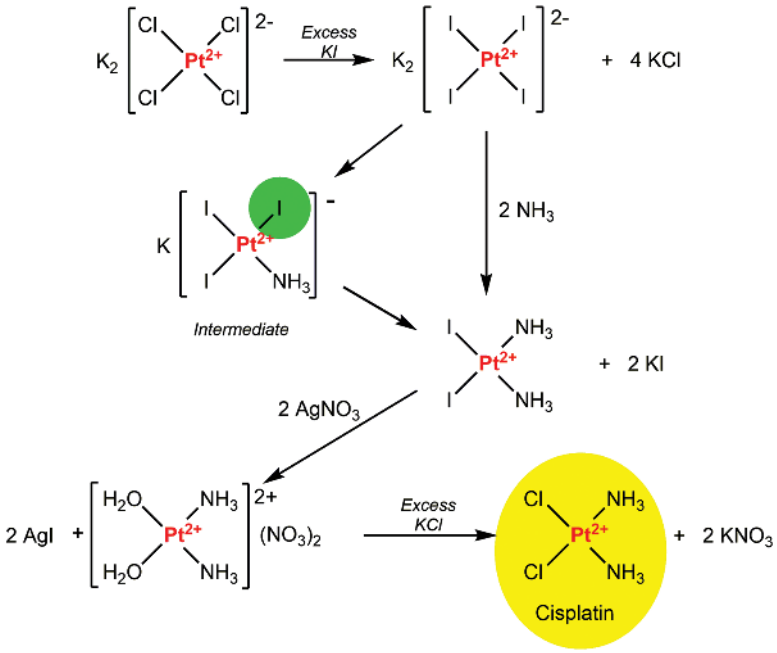


**Figure 1.24**
Dhara synthesis of cisplatin.

only the *cis* isomer is formed in the reaction. The key intermediate, which is normally not isolated in this reaction, is $[PtI_3(NH_3)]^-$ (Figure 1.24). The addition of the second equivalent of ammonia to this intermediate can proceed by displacing the iodide ion *trans* to the ammonia, or it can proceed by displacing one of the two iodides that are *cis* to the ammonia. If the displacement were purely random, one might expect 67% *cis* (there are two ways to make this isomer) and 33% *trans* (there is one way to make this isomer), but the isolated product is *100% cis*! This observation is a manifestation of the *trans* effect, which shows that the ability of iodide to direct substitution *trans* to itself is greater than that of ammonia to direct substitution *trans* to itself. Thus, as the reaction proceeds, the iodide ion that is *trans* to the other iodide is lengthening its bond, and it is eventually displaced from the platinum by ammonia to form the *cis* product, *cis*-$[PtI_2(NH_3)_2]$.

The next step in the Dhara synthesis is to replace the two iodides with two water molecules. This is done by adding two equivalents of silver nitrate, $AgNO_3$, which results in the formation of insoluble AgI. This reaction works because all metal complexes in aqueous solution exist in an equilibrium, which means that some fraction of the ligands bound to the metal ion must be in equilibrium with their unbound counterparts (Figure 1.25). If the complex is thermodynamically very stable, the equilibrium will be largely in favor of the intact complex, but the concentration of *unbound ligand* can never be zero. The equilibrium expressions (Figure 1.25) in the case of *cis*-$[PtI_2(NH_3)_2]$ are written as dissociations (dissociation of $I^-$ from platinum), and are described by the dissociation constant, $K_d$, which is related to the normal (association) equilibrium constant, $K$, by Eq. (1.26):

$$K = 1/K_d \tag{1.26}$$

While $K_{d1}$ and $K_{d2}$ (Figure 1.25) for this reaction are likely very small, the addition of $Ag^+$ ion to the solution as $AgNO_3$, which is water-soluble, causes insoluble AgI to

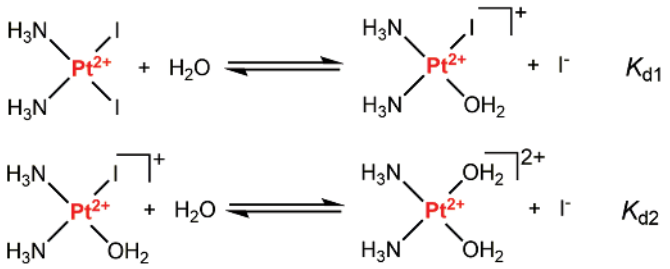


**Figure 1.25**
Equilibria involving the iodo complexes in the synthesis of cisplatin.

precipitate from solution; from Le Chatelier's principle, this drives the equilibrium to the right. This phenomenon is called a *phase change*, in which some of the material originally in the solution phase, $Ag^+$ and $I^-$, moves to a another phase, in this case insoluble AgI. Because the nitrate ion, $NO_3^-$, is lower in the spectrochemical series (see Table 1.2) than water, and the concentration of water is very high, >50 *M*, nitrate ion is simply a 'spectator ion' and is not part of the equilibrium expressions given in Figure 1.25.

The last step in the synthesis is to simply displace the two coordinated water molecules of *cis*-$[Pt(H_2O)_2(NH_3)_2]^{2+}$ by adding an excess of chloride ion as KCl, which forms yellow cisplatin, *cis*-$[PtCl_2(NH_3)_2]$. Even though $\Delta_o(H_2O) > \Delta_o\ (Cl^-)$, the addition of excess chloride ion to the medium drives the equilibrium to the right, and since cisplatin is only sparingly soluble in water, the complex precipitates from solution as its sparingly soluble dichloro form.

The synthesis of *transplatin* (Figure 1.26) also presents examples of the *trans* effect in coordination chemistry. As with cisplatin, the starting material for the synthesis of transplatin is $K_2[PtCl_4]$ which, in this case, reacts with excess ammonia to produce the tetra-ammine complex, $[Pt(NH_3)_4]^{2+}$. The next step is to react this complex with excess chloride ion in hot hydrochloric acid, HCl. In this reaction, the first chloride ion displaces

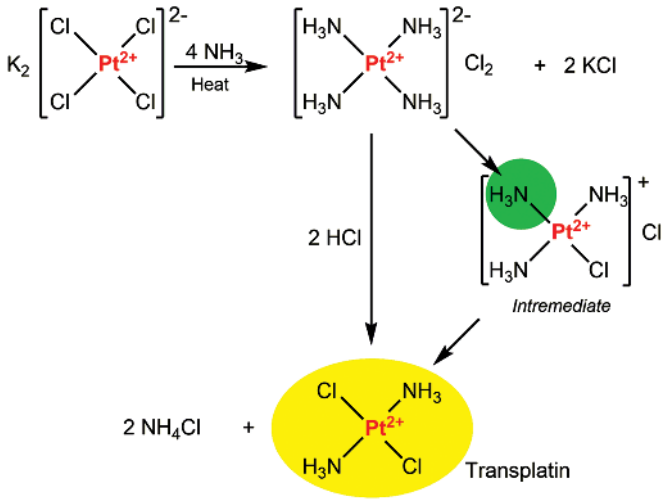


**Figure 1.26**
Synthesis of transplatin.

an ammonia molecule from platinum which, because the solution is very acidic, is immediately protonated to form $NH_4^+$. Since the lone pair on $NH_4^+$ is bound by a proton, the released ammonia molecule is blocked from attacking the platinum ion. The second chloride can either occupy the position *trans* to the first chloride or one of the two positions *cis* to the first chloride. Since the *trans* effect series shows that chloride is a better *trans* directing ligand than is ammonia (Table 1.5), the second chloride displaces the ammonia molecule *trans* to the first chloride to produce transplatin. While the reaction conditions would almost certainly lead to further displacement of ammonia from platinum by chloride, transplatin is the least soluble component in the reaction medium and it precipitates from the medium before it has the chance to further react with chloride ion.

### 1.6.5 Stability of Metal Complexes

One of earliest observations concerning the stability of metal complexes was the finding that for a given ligand set, such as water, complex stabilities for the first-row transition metals are in the order, $Mn^{2+} < Fe^{2+} < Co^{2+} < Ni^{2+} < Cu^{2+} > Zn^{2+}$, which became known as the *Irving Williams series*. This order is rationalized by considering the values of CFSE for high-spin (weak field) complexes which maximizes at $Ni^{2+}$ and is zero for $Mn^{2+}$ and $Zn^{2+}$ (Table 1.3). The maximum position of $Cu^{2+}$ in this series in due to the fact that $d^9$ has a significant Jahn–Teller distortion (see Figure 1.5; Section 1.4) which results in a tetragonal distortion making it more stable than the remaining complexes that have structures closer to the pure octahedron.

The important parameter in characterizing the stability of metal complexes is called the *stability constant*, $K$, or the *formation constant*, $K_f$. In certain cases, the stability of a complex is sensitive to pH, especially in the physiological range, in which case the *conditional stability constant*, at some specified condition, can be indicated. While there are many different ways to determine the stability constant of a metal complex, one is to use absorption spectroscopy to measure spectral changes in solution as ligand is added to the system. For example, consider the equilibrium binding process in Eq. (1.27), in which one ligand reacts with a metal ion to produce a 1:1 complex. The stability constant (equilibrium constant) for this system is given by Eq. (1.28), where [ML] is the concentration of complex and [M] and [L] are the concentrations of *free metal ion* and *free ligand*, respectively:

$$M + L = ML \tag{1.27}$$

$$K = \frac{[ML]}{[M][L]} \tag{1.28}$$

The typical way to determine the stability constant, $K$, for this system is to first determine the molar extinction coefficient of the complex that forms, ML, by driving the system to the right by adding a large excess of the ligand which complexes all of the metal ion. Once $\varepsilon_{max}$ for the complex is determined (see Box 1.2), solutions with different concentrations of ligand and a constant concentration of metal ion are prepared and their absorption spectra measured to determine the concentration of complex, ML, in each. By knowing the concentration of ML present in each mixture and the total concentrations of metal ion and ligand in the mixtures, the value of $K$ can be calculated from Eq. (1.28).

Most systems are much more complicated than the example given, and more than one equilibrium expression is most often involved. For example, consider the reaction of ammonia, $NH_3$, with the aquated complex $[Cu(H_2O)_6]^{2+}$. Since $Cu^{2+}$ has the electronic configuration $3d^9$, it is a Jahn–Teller distorted system with two of the *trans* water molecules on

the z-axis of the complex farther away from the metal ion than the other four. Studies using absorption spectroscopy show that in water, ammonia adds to aquated $Cu^{2+}$ in a stepwise manner to produce four distinct complexes, a process summarized by Eqs (1.29)–(1.32). Unless very unusual circumstances are present, the highest-order complex that forms in the ammonia system is $[Cu(NH_3)_4]^{2+}$, so for simplicity the two weakly-bound water molecules in the axial sites of $[Cu(H_2O)_6]^{2+}$ have been eliminated in the equilibrium reactions:

$$[Cu(H_2O)_4]^{2+} + NH_3 = [Cu(NH_3)(H_2O)_3]^{2+} + H_2O \quad (1.29)$$

$$[Cu(NH_3)(H_2O)_3]^{2+} + NH_3 = [Cu(NH_3)_2(H_2O)_2]^{2+} + H_2O \quad (1.30)$$

$$[Cu(NH_3)_2(H_2O)_2]^{2+} + NH_3 = [Cu(NH_3)_3(H_2O)]^{2+} + H_2O \quad (1.31)$$

$$[Cu(NH_3)_3(H_2O)]^{2+} + NH_3 = [Cu(NH_3)_4]^{2+} + H_2O \quad (1.32)$$

The equilibrium expression for the first step in this sequence is Eq. (1.33) which, if the concentration of water is eliminated in the reaction (it is a constant and is incorporated into $K$), gives Eq. (1.34):

$$\frac{[[Cu(NH_3)(H_2O)_3]^{2+}][H_2O]}{[[Cu(H_2O)_4]^{2+}][NH_3]} = K_1' \quad (1.33)$$

$$\frac{[[Cu(NH_3)(H_2O)_3]^{2+}]}{[[Cu(H_2O)_4]^{2+}][NH_3]} = K_1 \quad (1.34)$$

The equation which describes the formation of the final complex, called the *overall reaction*, from the free aqua complex and the free ligand is Eq. (1.35). By writing the individual equilibrium expressions in Eqs (1.29)–(1.32) to obtain $K_{1–4}$, it would be easy to show that the equilibrium constant for the overall reaction in Eq. (1.35) is the *product* of the individual stepwise equilibrium constants; that is Eq. (1.36). This product is given the designation $K_{1–n}$ or $\beta_n$, where n is the number of steps in the overall reaction. Since the values of $K_{1–n}$ and $\beta_n$ are often very large, the typical way to denote the overall stability constant is log $K_{1–n}$ or log $\beta_n$:

$$[Cu(H_2O)_4]^{2+} + 4NH_3 = [Cu(NH_3)_4]^{2+} \quad (1.35)$$

$$\frac{[[Cu(NH_3)_4]^{2+}]}{[[Cu(H_2O)_4]^{2+}][NH_3]^4} = K_1K_2K_3K_4 = K_{1-4} = \beta_4 \quad (1.36)$$

By systematically increasing the total concentration of ammonia in solution, collecting absorption spectra and fitting the data to a model, the stability constants for the copper–ammonia system at 30 °C were determined to be $K_1 = 1.78 \times 10^4\ M^{-1}$, $K_2 = 2.30 \times 10^3\ M^{-1}$, $K_3 = 9.77 \times 10^2\ M^{-1}$, and $K_4 = 63.1\ M^{-1}$, which in this case gives $K_1 \times K_2 \times K_3 \times K_4 = K_{1–4} = \beta_4 = 2.5 \times 10^{12}\ M^{-4}$, or log $K_{1–4}$ or log $\beta_4 = 12.4$ [8]. Note that while the unit of concentration is indicated in the values of $K$ and $\beta$, which is helpful for determining whether the equilibrium expression is written as an *association* or a *dissociation*, it is not possible to take the logarithm of the unit. As pointed out in Section 1.6.1, the concentration of a substance is assumed to be equal to the activity of the substance which, since the latter is unitless, will not present a problem in obtaining the logarithm of the value.

Similarly to Eq. (1.17), the relationship between the stability constant of the overall reaction, $K_{1–4}$ ($\beta_4$), and $\Delta G$ is given by Eq. (1.37), which is related to the change in enthalpy,

$\Delta H$, making and breaking bonds, and the entropy, $\Delta S$, the amount of disorder in the reaction, through the well-known Eq. (1.38):

$$K_{1-4} = \beta_4 = e^{-\frac{\Delta G}{RT}} \tag{1.37}$$

$$\Delta G = \Delta H - T\Delta S \tag{1.38}$$

### 1.6.6 Chelate Effect

For many years, scientists have recognized that ligands which form a ring structure that includes the metal ion, called a *chelate ring*, have exceptional thermodynamic stability. This 'extra' stability, beyond that which would be achieved with a similar system without a chelate ring, is called the *chelate effect* in inorganic chemistry. As with organic chemistry, chelate rings that have a total of five or six atoms in the ring (this includes the metal ion) are more stable than rings with four or seven members. In order to see how the chelate effect works, consider the reaction of two ammonia molecules with aquated $Cu^{2+}$ [Eq. (1.39)] and, for comparison, the reaction of the bidentate ligand, ethylenediamine, $NH_2CH_2CH_2NH_2$, abbreviated 'en', with aquated $Cu^{2+}$ [Eq. (1.40)].

$$[Cu(H_2O)_6]^{2+} + 2\,NH_3 \rightleftharpoons [Cu(H_2O)_4(NH_3)_2]^{2+} + 2\,H_2O \tag{1.39}$$

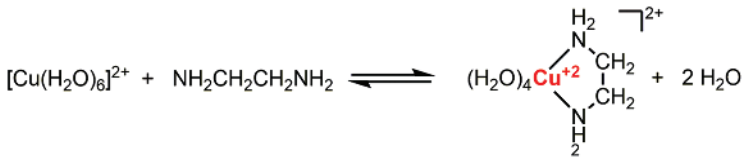


(1.40)

Experimentally, the reaction with ammonia [Eq. (1.39)] has an overall stability constant for formation of the *bis*-ammonia complex of $\log \beta_2 = 7.61$, while the reaction with en [Eq. (1.40)], which results in the formation of a five-membered, en, chelate ring, has $\log \beta_1 = 10.73$ at 25 °C [9]. This is an example of the chelate effect, in that the presence of the ring increases the stability constant of the $Cu^{2+}$–en complex over that of the $Cu^{2+}$ ammonia system by more than three orders of magnitude.

The nomenclature used when referring to the type of chelate ring formed by a ligand is to say the ligand is *bidentate* if it has two points of attachment (two donor atoms) to the metal ion, *tridentate* if it has three points of attachment, *tetradentate* if it has four, and so on. While the arrangement of chelate rings, the nature of the donor atoms and their charge, and the size of the rings all affect the stability of the complex, ligands which have multiple points of attachment to the metal ion generally produce the most stable complexes. An example of a common *hexadentate* ligand which forms very stable complexes with a wide variety of metal ions is EDTA, ethylenediaminetetraacetic acid (Figure 1.27).

The exceptional stability of metal chelate compounds implies that the binding constant of the ligand toward the metal ion, $K$, is large, and therefore the change in the free energy, $\Delta G$, through Eq. (1.17) is large and negative. Since $\Delta G$ is related to $\Delta H$ and $\Delta S$ through Eq. (1.38), it is sometimes possible to determine which thermodynamic quantity makes the most important contribution to the free energy. However, since $\Delta H$ and $\Delta S$ reflect the *net changes* in these quantities in the reaction, and solvent molecules around the starting materials and products can play an important role, even a qualitative assessment of the relative importance of these quantities is challenging. The fact that there are two 'particles' on the left of Eq. (1.40), the aquated complex and the bidentate ligand, and three particles

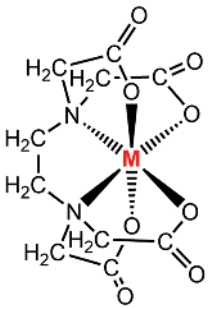


**Figure 1.27**
Structure of an octahedral complex with ethylenediaminetetraacetic acid, EDTA, which binds to the metal ion as a tetravalent anion.

on the right, the bidentate complex and two water molecules – the latter returning to bulk solvent – an increase in *entropy* in moving from left to right ($\Delta S$ is positive for the reaction) is often cited as the thermodynamic basis for the chelate effect.

## Box 1.4 Geometric and Optical Isomerism of Metal Complexes

The octahedron, which is the most common geometry of metal complexes, is made by joining eight identical equilateral triangles at their edges, which produces eight *faces* – the triangles – and six vertices – the points where four different triangles meet. If there are three identical bidentate ligands attached to the metal ion and the ligands have identical donor atoms on both 'ends', the complex formed is a *tris*-bidentate chelate compound containing three A–A-type ligands. An example of such an octahedral complex is $[Co(en)_3]^{3+}$, which contains three coordinated ethylenediamine (en) ligands. When three A–A-type ligands are attached to the metal ion, *two* of the faces of the octahedron are unique in that they have *three* different attached ligands, while the remaining six faces have only have *two* different attached ligands. The two unique faces, which are opposite each other on the octahedron, are shown as a dashed and a solid triangle in Figure 1.28.

An interesting property of a tris-bidentate chelate complex is that, even though the ligands themselves have no chiral centers (the ligands are not optically active), the arrangement of the three chelate rings on the octahedron produces a structure that has a nonsuperimposable mirror image; that is, the chelate ring system makes the compound chiral and there are two *enantiomers*. Inorganic chemists decided that the best way to specify the spatial arrangement of the bidentate ligands on the octahedron, which is called the *absolute configuration*, is to orient the enantiomer so that the eye of the observer is positioned above one of the unique faces; this view is shown on the right of Figure 1.28. In this case, the observer is looking along an *axis of symmetry* of the enantiomer, called the $C_3$ *axis of rotation* (rotation by 120°), and the second unique face appears as a triangle on the 'backside' of the structure. If the structure is rotated so that the back face is positioned toward the observer and the face that was originally toward the observer is at the back, the view of the structure will be identical to the

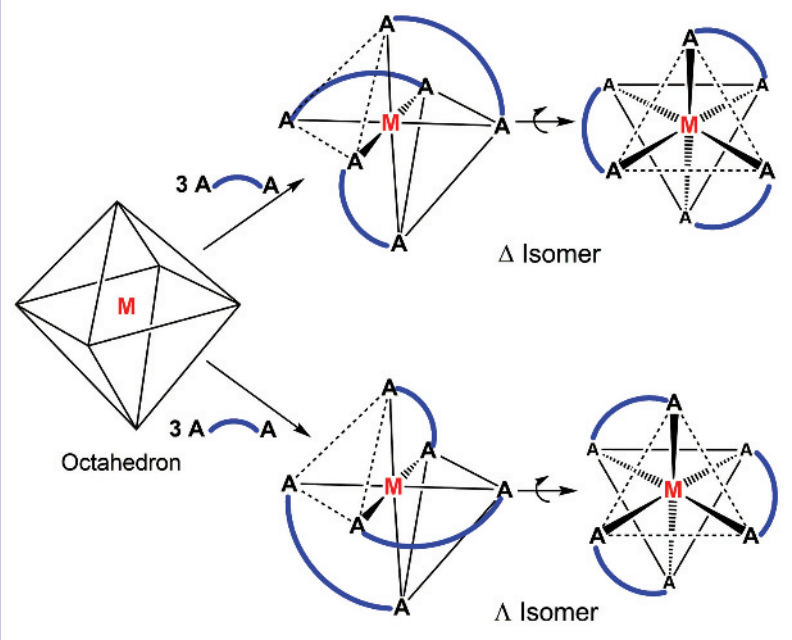


**Figure 1.28**
Optical isomers and absolute configuration for an octahedral tris-bidentate chelate complex with three identical symmetrical, bidentate, A–A-type ligands. Examples of commonly found A–A-type ligands are ethylenediamine, $NH_2CH_2CH_2NH_2$, A = N, oxalate, $O_2CCO_2^{2-}$, A = O, and so on.

original view; that is, the enantiomer looks the same when viewed from either unique face. The assignment of absolute configuration of an enantiomer is made by noting the 'sense' of the chelate rings in passing from the front to the back of one of the unique faces. If when passing from the front to the back the chelate rings trace out motion in a *clockwise* direction – that is, the rings conform to a right-hand spiral or a right-hand screw or propeller – the enantiomer is assigned the Δ *absolute configuration*. If, on the other hand, in moving from the front to the back of the structure the observer sees the rings trace out a *counter-clockwise* motion – that is, the rings conform to a left-hand spiral or left-hand screw or propeller – the enantiomer is assigned the Λ *absolute configuration.* These two possibilities, with views above one of the two unique faces of the Λ and Δ enantiomers, are shown in Figure 1.28.

While the above convention is used to determine the absolute configuration of all tris-bidentate chelate complexes, ligands that have donor 'ends' that are not the same also produce structural (geometric) isomers, each of which exists in mirror-image pairs. For example, the anion of the amino acid glycine, glycinate (gly), $NH_2CH_2CO_2^-$, which is a good chelating agent, forms a five-membered chelate ring with a metal ion. Since this ligand uses the nitrogen atom of the amino group and an oxygen atom of the carboxyl group to bind to a metal ion to form a chelate ring, it is an unsymmetrical, A–B-type ligand. As a consequence of this *asymmetry*, the complex $[M(gly)_3]$, and others like it that have three A–B-type ligands, exists in *two geometric forms*, both of which have nonsuperimposable mirror images. The name of the

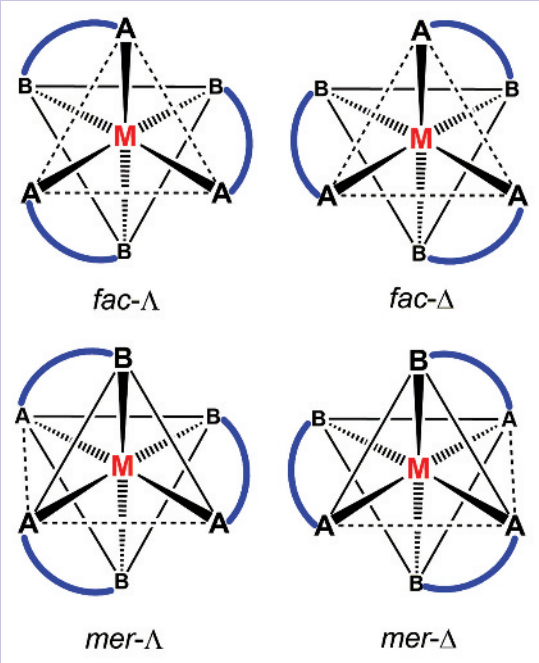


**Figure 1.29**
Geometric and optical isomers for octahedral tris-bidentate chelate complexes with three identical, unsymmetrical, A–B-type ligands. Examples of commonly found ligands of this type are glycinate, $NH_2CHCO_2^-$, where A = N and B = O, di-deprotonated glycolic acid, $^-OCH_2CO_2^-$, A = O(OH), B = $O(CO_2H)$, and so on. The front unique face for the *fac* isomer and the edge, meridian, for the *mer* isomer are shown with dashed lines.

geometric isomer is determined by the location of donor atoms from each of the attached ligands. As shown in Figure 1.29, one geometric isomer has three 'A' donors from *three different ligands* on one face of the octahedron and three 'B' groups on a second face. This geometric isomer is designated the *facial* or *fac* isomer, indicating that common donors from the three ligands occupy a face (actually two faces) of the octahedron. The second geometric isomer (there are only two) is one that has common donor atoms from each of the three ligands on the *edge* or *meridian* of the octahedron, which is the *mer* isomer. As shown in Figure 1.29, both the *fac* and the *mer* geometric isomers also have a nonsuperimposable mirror image, which means that there are a total of four isomers: two geometric isomers each of which exists as an enantiomeric pair. As with the symmetrical A–A ligand, the absolute configurations of these isomers is determined by finding one of the two faces with three different attached ligands (note that the front face for the *mer* isomer has two As and one B from the three ligands), positioning the observer above the face and determining the 'sense' of the chelate rings – either right-hand, Δ, or left-hand, Λ – in passing from the front to the back of the structure.

Organic ligands that can be attached to a metal ion have a wide variety of different structures, and while it is not possible to cover all of isomeric possibilities that

might be encountered, some general comments concerning the sources of geometric and optical isomerism can be made. Some bidentate ligands have identical donor atoms – for example, both atoms could be O or both could be N – but the organic structure connecting the two donor atoms in some way distinguishes the two 'ends' of the ligand. For example, one O-donor could be a deprotonated alcohol functional group and the other could be the oxygen atom of a deprotonated carboxylic acid functional group, as would occur with di-deprotonated glycolic acid, $^{-}OCH_2CO_2^{-}$. While both donor atoms are oxygen, the two ends of the ligand are clearly not the same. In this case, two different orientations of the ligand on the metal are possible and, depending on the nature and number of other ligands bound to the metal, geometric isomers might be present. Sometimes, octahedral complexes have only two chelate rings, with the remaining two sites being occupied by monodentate ligands, which do not generate a ring. If the monodentate ligands are *cis* to one another on the octahedron, the two chelate rings cause the resulting structure to have nonsuperimposable mirror images; that is, the compound exists as enantiomeric pairs. Determining the absolute configuration in this case is done by simply matching the sense of the chelate rings of the bis-bidentate compound with the tris-bidentate examples shown in Figures 1.28 and 1.29. Often, the ligands attached to the metal ion contain chiral centers and are themselves optically active, for example amino acids. Placing ligands of this type in an octahedral environment around a metal ion can give rise to even more complex isomeric possibilities involving the relative arrangement of the donor atoms on the octahedron, the absolute configurations of the asymmetric atoms in the ligand, and the absolute configuration of the ring system.

While all of this may seem to be on the fringe of what one needs to know about metal complexes that have found their way into medicine, it is important to point out that the biological system is a very chiral environment. Proteins are made up of amino acids, which have chiral centers; nucleic acids have chiral sugars; and the DNA double helix is chiral. Suppose, for example, a racemic metallo-drug is administered to the body and both enantiomers become bound to a target molecule to produce Δ-drug–target and Λ-drug–target. Since these two adducts are *diastereomeric* to one another (not exact mirror images of each other), they will not have the same physical properties, and most likely the binding constants of the Δ and Λ drug enantiomers toward the chiral target will not be the same. Since the strength of a drug–receptor interaction at the molecular level is often the basis for biological activity, choosing the correct optical isomer may mean the difference between high biological activity and none at all [10].

### 1.6.7 Macrocyclic Effect

As might be expected, totally surrounding the metal ion with a ligand that is cyclic and has no 'ends' further enhances the stability of the resulting complex. For example, consider the complexes $[Cu(232\ tet)]^{2+}$ and $[Cu(cyclam)]^{2+}$, shown in Figure 1.30, which are formed in the reaction of aquated $Cu^{2+}$ with the *acyclic ligand*, 232 *tet*, or the *macrocyclic ligand*, *cyclam*. The stability constant for $[Cu(232\ tet)]^{2+}$ at 25 °C is $\log \beta_1 = 23.2$, while the stability constant for $[Cu(cyclam)]^{2+}$ is $\log \beta_1 = 27.2$ [11]. The observation that the stability constant for a complex containing a macrocyclic ligand is greater than the stability constant

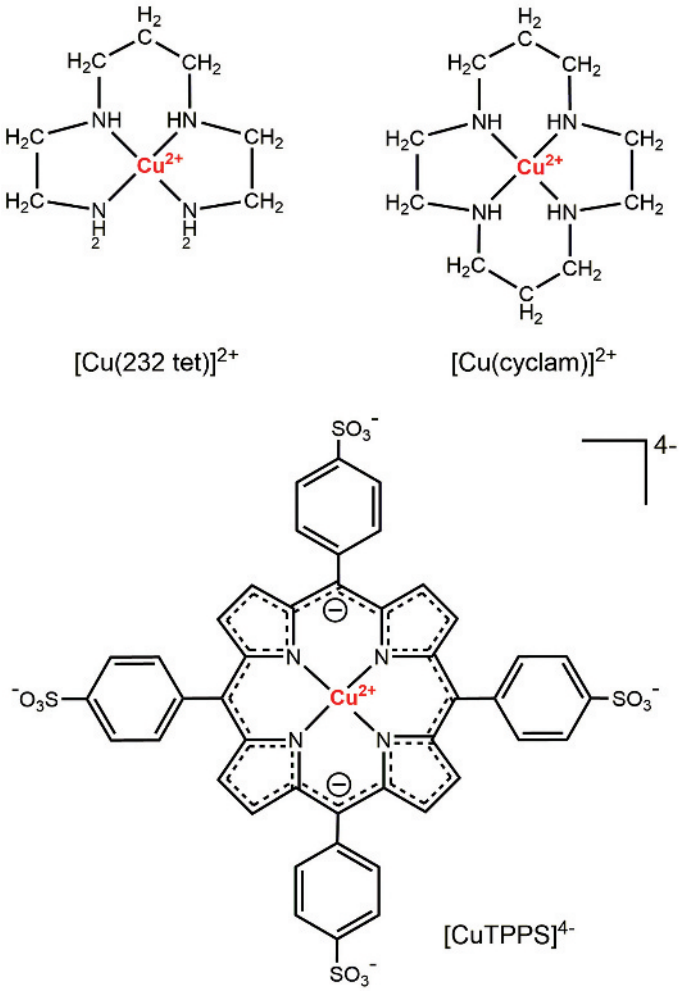


**Figure 1.30**
Structures of $[Cu(232\ tet)]^{2+}$, $[Cu(cyclam)]^{2+}$ and [Cu(TPP)], where TPP is the di-deprotonated porphyrin core of *meso*-tetra-(*p*-sulfonatophenyl)porphyrin.

for an analogous complex with an acyclic ligand is termed the *macrocyclic effect* in inorganic chemistry. The values of $\Delta H$ for $[Cu(232\ tet)]^{2+}$ and $[Cu(cyclam)]^{2+}$ are –110.8 and –135.4 kJ $mol^{-1}$, respectively, clearly showing that enthalpy contributes to the enhanced stability of the macrocyclic complex. The values of $\Delta S$ for the two compounds are 66.9 and 50.2 J $mol^{-1}$ $K^{-1}$, respectively, showing that entropy actually favors formation of the acyclic complex, $[Cu(232\ tet)]^{2+}$. Although it is not easy to explain the observed values of $\Delta H$ and $\Delta S$ from the structures of the complexes alone, or what might be taking place in terms of bond breaking and formation and what the 'order/disorder' (entropy change) is like on either side of the reaction, the macrocyclic effect appears to be largely governed by *enthalpic* factors.

The porphyrin ligand, which is present in many biological molecules, is a highly versatile tetraaza (four nitrogen atoms) macrocyclic ligand which forms very stable complexes. In

the free form, the porphyrin ligand has two pyrrole hydrogen atoms, which can be lost when the ligand, as a dianion, binds to a metal ion. For example, the reaction of $Cu^{2+}$ with the *tetra* sulfonated porphyrin ligand TPPS produces the complex, $[Cu\text{-}TPPS]^{4-}$ (Figure 1.30). This complex, which has a stability constant at 25 °C of $\log \beta_1 = 38.1$, is considerably more stable than $[Cu(cyclam)]^{2+}$ [12]. Although detailed thermodynamic data for Cu-TPPS are not available, the high stability of the complex is likely due to the fact that the porphyrinato ligand has two negative charges and thus is electrostatically attracted to the metal ion, which is a cation. An additional factor underlying the stability of $[Cu\text{-}TPPS]^{4-}$ is probably related to the high rigidity of the porphyrin macrocycle. Once a metal ion is bound in the cavity of the ligand, removing the porphyrin requires folding the structure in some manner that would be energetically very unfavorable. Thus, highly conjugated, aromatic, porphyrin ligands enhance the macrocyclic effect to an even higher level than other types of macrocyclic structure.

### 1.6.8 Hard–Soft Acids–Bases

The concept of hard and soft acids and bases, given the acronym HSAB, was introduced by the renowned inorganic chemist Ralph G. Pearson [13]. This concept addresses the rate of formation and thermodynamic stability of metal complexes in terms of the nature of the metal ion and ligand that come together to form a bond. Pearson observed that a metal ion which is a so-called 'hard acid' forms a strong complex with a ligand that is a 'hard base,' and a metal ion that is a 'soft acid' also forms a strong complex with a ligand that is a 'soft base.' If the bonding partners are interchanged – that is, soft acid with hard base or hard acid with soft base – complexes with lower stabilities result. This early remarkable observation was based on the measured rates and stabilities of complexes and on an assessment of the 'deformability or polarizibility' of the 'electron clouds' on both the metal ion and the ligand. If a metal ion or ligand has a large radius and low net charge, the nucleus has less control over the frontier (outer) electrons and the electron distribution of the ion can be more easily distorted (polarized). A metal ion or ligand donor atom with these properties is considered a *soft acid* (M) or *soft base* (L). If, on the other hand, an ion has a high charge and a small radius, the electronic shape of the ion cannot be easily polarized or distorted. A metal ion or ligand with these properties is considered a *hard acid* (M) or a *hard base* (L). While the observation of which combinations produce the highest stabilities and reaction rates is irrefutable, explaining the effect in terms of the physical properties of atoms and ions is not straightforward and is beyond the scope of the presentation given here.

One point concerning the connection between the rate of a reaction (a kinetic property) and the stability of a compound (a thermodynamic property) is worth noting. From transition state theory, the rate constant for a reaction depends in an inverse exponential way on the activation free energy of the reaction, $\Delta G^{\ddagger}$, through Eq. (1.22). On the other hand, the stability constant for the products formed in the reaction, $K$, is determined from the differences in the free energies of the products and reactants, $\Delta G_{rxn}$, through Eq. (1.17). Using the principles of transition state theory, this means that if $\Delta G_{rxn}$ is large and negative, $\Delta G^{\ddagger}_{f}$ is small and positive and the rate constant, $k$, for reactants moving to products is large [Eq. (1.22)]. In the context of the HSAB concept, this means that if all other factors are equal, a soft ligand will react *faster* with a soft metal ion to produce a complex with high stability, while a hard ligand will react with a soft metal ion more *slowly* to produce a complex with low stability.

**Table 1.6** Hard–soft acids–bases.

| Metal ions (Acids) | | | Ligands (Bases) | | |
|---|---|---|---|---|---|
| Soft | Intermediate (Borderline) | Hard | Soft | Intermediate | Hard |
| $Au^{+}$ | $Au^{3+}$ | $Tc^{5+}$, $Tc^{7+}$ | CN-R | Pyridine | $H_2O$ |
| $Tc^{+}$ | $Ru^{3+}$ | $Gd^{3+}$ | CO | Imidazole | $HO^{-}$ |
| $Pt^{2+}$ | $Ti^{2+}$ | $Ga^{3+}$ | $R\text{-}S^{-}$ | $Br^{-}$ | acac |
| $Pt^{4+}$ | $Fe^{2+}$ | $Ti^{4+}$ | $R_2S$ | | $NH_3$ |
| $Cu^{+}$ | $Zn^{2+}$ | $Fe^{3+}$ | Cp | | $RNH_2$ |
| $Ru^{2+}$ | $Cu^{2+}$ | $Re^{5+}$, $Re^{7+}$ | $R_3P$ | | $R_2NH$ |
| $Re^{+}$ | $Tc^{3+}$ | $V^{4+}$, $V^{5+}$ | DMSO | | $Cl^{-}$ |
| $Ag^{+}$ | $Re^{3+}$ | $Li^{+}$ | $CN^{-}$ | | $CO_3^{2-}$, $HCO_3^{-}$ |
| $As^{+}$, $As^{3+}$ | $Sb^{3+}$ | $Mn^{2+}$ | $AsR_3$ | | $H_2PO_4^{-}$, $HPO_4^{2-}$ |
| $Pd^{2+}$ | $Bi^{3+}$ | $Sb^{5+}$ | | | $RCO_2^{-}$ |
| | $Co^{2+}$ | $Co^{3+}$ | | | $O^{-2}$ |
| | $Rh^{3+}$ | $Ca^{2+}$ | | | |
| | $Ir^{3+}$ | $Sr^{2+}$ | | | |
| | $Os^{2+}$ | $Sn^{4+}$ | | | |
| | | $Si^{4+}$ | | | |

| Ligands (Bases) on DNA/RNA | | | Ligands (Bases) on Proteins | | |
|---|---|---|---|---|---|
| Soft | Intermediate | Hard | Soft | Intermediate | Hard |
| | Nitrogen sites on, A, G, T, C, U | $[ROPO_2OR]^{-}$ | $R\text{-}S^{-}$, Cys | Imidazole | $RNH_2$, Lys |
| | | | $RSCH_3$, Met | RSSR, Disulfide | $RCO_2^{-}$, Asp, Glu |
| | | | $RS^{-}$, GSH | | $\phi\text{-}O^{-}$, Tyr |
| | | | $R\text{-}Se^{-}$, Sec | | $R\text{-}O^{-}$, Ser, Thr |

Cp, cyclopentadienyl; DMSO, dimethylsulfoxide; acac, acetylacetone; GSH, glutathione.

While the exact reasons why hard–hard and soft–soft combinations are better than hard–soft/soft–hard combinations is challenging to explain, simply knowing which combinations lead to products with high stabilities and rates of formation is very useful for assessing whether and to what extent a metal complex introduced into the body will react with nucleophiles found in the biological milieu. A list of the hard–soft acids–bases to be encountered in this text is given in Table 1.6.

## 1.7 Summary

Most of the metal complexes that are used for treating or detecting disease are coordination compounds. The description of the bonding in these compounds, referred to as crystal field (CF) theory, involves electrostatic interactions between charges or dipoles on the attached ligands and the cationic metal ion, which lifts the fivefold degeneracy of the *d*-orbitals on the metal ion. The most common geometry is an octahedral array of six ligands bound to the metal ion that splits the *d*-orbital set into $t_{2g}$ and $e_g$ levels that are separated in energy by $\Delta_o$, the crystal field splitting parameter. Adding electrons to the octahedral splitting pattern results in different degrees of compound stabilization, referred to as the crystal field stabilization energy, CFSE, and changing the number and arrangement of ligands produces

different *d*-orbital splitting patterns reflective of compound structure. The *d*-orbital splitting, which is controlled by the nature of the ligands through the spectrochemical series, the principal quantum number of the *d*-orbitals and the oxidation state of the metal ion, explains the spectral and magnetic properties of coordination compounds.

While CF theory is useful tool for analyzing bonding, molecular orbital (MO) theory provides a broader-based description of bonding in metal-containing compounds. Organometallic chemistry, a major branch of inorganic chemistry, focuses on compounds having carbon-centered ligands bound to metal ions in low oxidation states. Bonding in these compounds – as well as in coordination compounds – can be described using MO theory, which provides a more comprehensive energy level diagram for metal-containing compounds.

Due to the presence of absorptions in the visible region of the spectrum, complexes containing transition metal ions are highly colored. Analysis of the absorption spectra of these compounds shows that the intensity and locations of absorption bands are governed by quantum mechanical selection rules and the crystal field splitting parameter $\Delta_o$. Using CF theory, it is possible to determine the magnitude of $\Delta_o$ from spectra, which provides useful information on the thermodynamic stability and chemical reactivity of the compound.

The most common reaction for a metal complex is the ligand substitution reaction in which a ligand originally bound to the complex is replaced by an attacking nucleophile. An important 'benchmark' reaction for estimating the rate at which a given metal ion may undergo a substitution reaction is the rate at which it exchanges one of its bound water molecule with a water molecule that is free in solvent. These water exchange rates span an enormous range – that is, $\sim$ 19 orders of magnitude – with crystal field effects dominating the slow-exchanging ions and electrostatic potential phenomena influencing the fast-exchanging ions.

One of the most important discoveries in coordination chemistry was the kinetic *trans* effect that specifies which ligand is lost in a substitution reaction involving square-planar complexes. This effect is at the center of how the anticancer drug cisplatin and its less active *trans* isomer are synthesized, and it plays a prominent role in the reactions of many metal–drug complexes in the biological milieu.

The overall equilibrium constant $K_n$ for a multistep association is the product of the individual steps in the process. This can be seen in the titration of aquated $Cu^{2+}$ with ammonia to form $[Cu(NH_3)_4]^{2+}$ in a stepwise manner, which in turn allows the determination of individual equilibrium constants $K_{1–4}$ ($\beta_4$) and $\Delta G$ for the overall reaction. A useful way to enhance the stability of a metal complex is to use multidentate ligands with the ability to form chelates rings with the metal ion. A special case of chelation involves macrocyclic ligands that completely encircle the metal ion, forming exceptionally stable metal complexes.

Octahedral tris-bidentate chelate complexes having symmetrical ligands can be resolved into optical isomers which, depending on the disposition of the chelate rings relative to the $C_3$ axis of the compound, have either a $\Lambda$ or $\Delta$ absolute configuration. Similar complexes with unsymmetrical bidentate ligands have two geometric isomers, either of which can be resolved into optical isomers. The main spectroscopic tools for studying optically active metal complexes are optical rotatory dispersion (ORD) and circular dichroism (CD). The former is used for determining the rotation of plane polarized light, while the latter measures the absorption of right or left circularly polarized light by the sample.

An easy and general way to estimate the relative stability of metal complexes is to use hard and soft acid and base (HSAB) concepts developed by Pearson. Complexes having easily polarized electronic distributions on both the metal ion and ligand and those with

nondeformable electronic distributions on the bonded pair, produce complexes with high stability relative to those compounds which have mismatched metal–ligand polarizabilities.

## Discussion Questions

**1** Discuss the significance of oxidation state as it pertains to the cobalt ions in $[Co(NH_3)_6]^{3+}$ and $[Co(CN)_6]^{3-}$. Inspection of the MO diagram for $[Co(NH_3)_6]^{3+}$ (Figure 1.10) shows that the 6 *d*-electrons in the $t_{2g}$ orbital set do not interact with any orbitals on the ligand side of the MO diagram, which means that electrons in these orbitals (there are six) spend 100% of their time on the cobalt ion, showing that the cobalt ion in the compound is really $Co^{3+}$. Contrast this with $[Co(CN)_6]^{3-}$ (MO diagram not shown) that has antibonding MOs on the $CN^-$ ligands strongly interacting with the $t_{2g}$ orbital set, causing the six electrons to spend, for example, 50% of their time on the ligands and 50% on the cobalt ion. Is the cobalt ion in $[Co(CN)_6]^{3-}$ really $Co^{3+}$, or is its so-called 'oxidation state' lower than $3^+$? Under what circumstances is the concept of oxidation state compatible with MO theory?

**2** Discuss the similarities and differences between the structures of the iron porphyrin in hemoglobin ($Fe^{3+}$ form; Figure 7.3) and the cobalt corrin in vitamin $B_{12}$ (Figure 5.8). The iron porphyrin complex in hemoglobin is used for oxygen transport, while the cobalt corrin in vitamin $B_{12}$ can be reductively activated to transfer alkyl radicals to a substrate. Why are these function so different? [see Geno, M.K. and Halpern, J. (1987) Why Does Nature Not Use the Porphyrin Ligand in Vitamin $B_{12}$? *J. Am. Chem. Soc.,* **109**, 1238–1240].

**3** The famous scientist Professor R.J.P. Williams made significant contributions to the field of inorganic chemistry, but especially to bio-inorganic chemistry. After reading the tribute to his career [Thomson, A.J. (2016) The science of R.J.P. Williams, *J. Biol. Inorg. Chem.*, **21**, 1–3], discuss two scientific discoveries made by Professor Williams that advanced the field of inorganic/bio-inorganic chemistry.

**4** Discuss why the color of octahedral $[Mn(H_2O)_6]^{2+}$ is pale pink, while the color of tetrahedral $[MnO_4]^-$ is an intense purple.

## Problems

**1** Give the number of *unpaired electrons* in the complexes $[Ni(en)_3]^{2+}$, octahedral, $[NiCl_4]^{2-}$, tetrahedral and $[Ni(CN)_4]^{2-}$, square planar. The abbreviation 'en' is $H_2NCH_2CH_2NH_2$ or ethylenediamine, which acts as a bidentate ligand with two points of attachment to the $Ni^{2+}$ ion.

**2** Of the following pairs of complexes, which one has the *larger* crystal field spitting parameter, Δ? Which complex of the pair has the absorption maxima of its *d-d* electronic transitions at *higher* energy? Give reasons for your choice.

**a.** $[CoF_6]^{4-}$ vs. $[CoF_6]^{3-}$

**b.** $[Fe(CN)_6]^{4-}$ vs. $[Os(CN)_6]^{4-}$

**c.** $[CoF_6]^{3-}$ vs. $[CoCl_6]^{3-}$

**d.** $[Co(H_2O)_6]^{2+}$ vs. $[CoCl_4]^{2-}$

**e.** $[TiF_6]^{3-}$ vs. $[VF_6]^{2-}$.

**3** Consider that $[Au\ Cl_4]^-$, $5d^8$, can exist in either of two possible geometries, square planar, $S = 0$ or tetrahedral, $S = 1$. Using the energies of the *d*-orbitals in Table 1.1, estimate the value of $P/\Delta_o$ at which both geometries, from crystal field considerations, would be *equally likely*.

**4** Determine the crystal field stabilization energy (CFSE, in units of $\Delta_o$ and $P$), and the electronic configuration, $t_2^3 e_g^1$ and so on, of the following. The quantity $S$, the total spin quantum number, is the number of unpaired electrons divided by 2.

**a.** $[FeBr_6]^{4-}$, octahedral, $S = 2$

**b.** $[Fe(CN)_6]^{4-}$, octahedral, $S = 0$

**c.** $[FeCl_4]^{2-}$, tetrahedral, $S = 2$.

**5** Draw and label the approximate molecular orbital diagrams for an octahedral complex with only σ-bonding between the metal ion and ligands. Indicate which levels in the diagram can be derived using simple crystal field splitting arguments.

**6** The magnetic moment for a metal complex is 3.92 BM. How many unpaired electrons are there on the metal ion in the complex?

**7** A complex of a first-row transition metal complex has an octahedral geometry with $S = 1$ and $\mu_{eff} = 3.42$ BM. Answer the following:

**a.** How many unpaired electrons does the complex have?

**b.** Briefly explain why $\mu_{eff}$ is greater than $\mu_{so}$ for this complex.

**8** The pseudo first-order rate constant for the reaction of the thiol-containing ligand glutathione with a metal complex is $1.2 \times 10^{-2}\ s^{-1}$ at 37 °C. If the concentration of thiol in the reaction medium is 1 m*M* and the concentration of metal complex is 1 μ*M*, calculate the *second-order rate constant* for the reaction from the data given.

**9** Carbonic anhydrase (CA) is a zinc-containing enzyme located in the cytoplasm and mitochondria that catalyzes the conversion of carbon dioxide to carbonic acid by reaction with water. If the concentration of carbon dioxide in solution decreases from 220 m*M* to 55.0 m*M* in $1.22 \times 10^4$ seconds, and the reaction is far from reaching equilibrium, calculate the $t_{1/2}$ (half life) for the first-order reaction.

**10** The DNA nucleotide adenosine triphosphate, ATP, reacts with the metal complex $[ML_3Cl]$ in aqueous media by loss of the chloride ligand according to the reaction below:

$$[ML_3Cl] + ATP = ML_3 - ATP + Cl^-$$

**a.** If the initial rate for this reaction is $3.6 \times 10^{-2}\ M\ s^{-1}$ at 37 °C and the initial concentration of both the nucleotide and the metal complex in the reaction medium is $3.0 \times 10^{-3}\ M$, calculate the *second-order rate constant*, $k_2$, for the reaction.

**b.** After 24 hours the reaction reaches equilibrium and the equilibrium constant, $K$, is determined to be $10^2$. Calculate the free energy, $\Delta G$, for the reaction $R = 8.314\ J\ K\ mol^{-1}$.

**c.** Calculate the second-order *reverse rate constant*, $k_{-2}$, to reform starting materials for the reaction.

**11** Using the *trans* effect series, predict the products of the following reactions. Assume a ratio of starting material to reactant of 1:1.

**a.** $[PtCl_3(CO)]^- + NH_3 \rightarrow$

**b.** $[PtBr_3(NH_3)]^- + NH_3 \rightarrow$.

**12** The reaction of a nucleophile with a metal complex produces two products, A and B, which are in equilibrium with each other with $[A]_{eq} = 2[B]_{eq}$ at 37 °C. Calculate the free-energy difference between A and B, $R = 8.314$ J K mol$^{-1}$.

**13** The equilibrium constants for the addition of the first and second ligand chloride ligand to a metal complex are $K_1 = 3.6 \times 10^4$ and $K_2 = 4.1 \times 10^3$. Calculate log $\beta_2$ for this complex.

**14** The linear two-coordinate $Au^+$ complex [AuCl($PEt_3$)], where $PEt_3$ is triethylphosphine, is implicated in the reactions of the anti-arthritic drug auranofin. When this complex reacts with nucleophiles by losing the chloride ligand, will it form a more stable complex with the $\varepsilon$-amino group ($NH_2$-R) of the amino acid lysine or the thiol group (HS-R) of the amino acid cysteine? Briefly explain your choice.

## References


1. Tinoco, I., Sauer, K., Wang, J.C., and Puglisi, J.D. (2002) Physical chemistry, in: *Principles and Applications in Biological Chemistry*, 4th edn, Prentice-Hall, Upper Saddle River, NJ.
2. Paul, A. (1975) Optical and ESR spectra of titanium (III) in $Na_2O$-$B_2O_3$ and $Na_2O$-$P_2O_5$ glasses. *J. Mater. Sci.*, **10**, 692–696.
3. Riordan, A.R., Jansma, A., Fleischman, S., *et al.* (2005) Spectrochemical series of Cobalt(III). An experiment for high school through college. *Chem. Educ.*, **10**, 115–119.
4. Helm, L. and Merbach, A.E. (1999) Water exchange on metal ions: experiments and simulations. *Coord. Chem. Rev.*, **187**, 151–181.
5. Chernyaev, I.I. (1926) The mononitrites of bivalent platinum. *I. Ann. Inst. Platine (USSR)*, **4**, 243–275.
6. Alderden, R.A., Hall, M.D., and Hambley, T.W. (2006) The discovery and development of cisplatin. *J. Chem. Educ.*, **83**, 728–734.
7. Dhara, S.C. (1970) A rapid method for the synthesis of cisplatin. *Indian J. Chem.*, **8**, 193–194.
8. Trevani, L.N., Roberts, J.C., and Tremanine, P.R. (2001) Copper(II)–Ammonia complexation equilibria in aqueous solutions at temperatures from 30 to 250°C by visible spectroscopy. *J. Solution Chem.*, **30**, 585–622.
9. Spike, C.G. and Parry, R.W. (1953) Thermodynamics of chelation. II. Bond energy effects in chelate ring formation. *J. Am. Chem. Soc.*, **75**, 3770–3772.
10. Waldbeck, B. (1993) Biological significance of the enantiomeric purity of drugs. *Chirality*, **5**, 350–355.
11. Liang, X. and Sadler, P.J. (2004) Cyclam complexes and their applications in medicine. *Chem. Soc. Rev.*, **33**, 246–266.
12. Jiméenez, H.R., Julve, M., Moratal, J.M., and Favs, J. (1978) Stability constants of metalloporphyrins. A study of the protonation, deprotonation, and formation of Copper(II) and Zinc(II) complexes of meso-tetra-(*p*-sulfonatophenyl) porphyrin. *J. Chem. Soc. Chem. Commun.*, 910–911.
13. Pearson, R.G. (1963) Hard and soft acids and bases. *J. Am. Chem. Soc.*, **85**, 3533–3539.


## Further Reading


Atkins, P. and De Paula, J. (2006) *Atkins' Physical Chemistry*, 8th edn, W. H. Freeman and Co., New York, NY.

Ebbing, D.D. and Gammon, S.D. (2009) *General Chemistry*, 9th edn, Houghton Miffli.

Housecroft, C.E. and Sharpe, A.G. (2007) *Inorganic Chemistry*, 3rd edn, Pearson Education Limited, Edinburgh Gate, UK.

Huheey, J.E., Keiter, E.A., Keiter, R.L. (1993) Inorganic chemistry, in: *Principles of Structure and Reactivity*, 4th edn, Benjamin-Cummings Publishing Co., San Francisco, CA.

Lever, A.B.P. (1968) *Inorganic Electronic Spectroscopy*, 1st edn, Elsevier Publishing Co., Amsterdam, Netherlands.
Lever, A.B.P. (1984) *Inorganic Electronic Spectroscopy*, 2nd edn, Elsevier Science Publishers B. V., Amsterdam, Netherlands.
Miessler, G.L. and Tarr, D.A. (2004) *Inorganic Chemistry*, 3rd edn, Pearson Prentice-Hall, Upper Saddle River, NJ.
Nakamoto, K. and McCarthy, P.J. (1968) *Spectroscopy and Structure of Metal Chelate Compounds*, John Wiley & Sons Inc., New York.
Strohfeld, K.A. (2015) Essentials of Inorganic Chemistry: For Students of Pharmacy, Pharmaceutical Sciences and Medicinal Chemistry, John Wiley & Sons Inc., Chichester, UK.